

Using scoring functions to evaluate point process forecasts

Jonas R. Brehmer

Heidelberg Institute for Theoretical Studies, Heidelberg, Germany

Tilmann Gneiting

Heidelberg Institute for Theoretical Studies, Heidelberg, Germany
Karlsruhe Institute of Technology, Karlsruhe, Germany

Martin Schlather

University of Mannheim, Mannheim, Germany

Kirstin Strokorb

Cardiff University, Cardiff, United Kingdom

March 22, 2021

Abstract

Point process models are widely used tools to issue forecasts or assess risks. In order to check which models are useful in practice, they are examined by a variety of statistical methods. We transfer the concept of consistent scoring functions, which are principled statistical tools to compare forecasts, to the point process setting. The results provide a novel approach for the comparative assessment of forecasts and models and encompass some existing testing procedures.

Keywords and phrases: Elicitability, scoring functions, consistency, point processes, forecast evaluation.

2010 MSC: Primary 62C05
Secondary 60G55

Contents

1	Introduction	2
2	Scoring functions and forecast evaluation	3
2.1	Preliminaries on scoring functions	3
2.2	Forecast comparison and score differences	5
2.3	Application to point process settings	6
3	Consistent scoring functions for point patterns	8
3.1	Technical context	8
3.2	Density and distribution – general processes	10
3.3	Intensity and moment measures	14
3.4	Summary statistics	17
3.5	Density and distribution – temporal processes	19

4	Review of extant methods for model comparison	22
4.1	Information gain	23
4.2	Earthquake likelihood model testing	24
4.3	Connections to scoring theory	25
5	Simulation examples	29
5.1	Intensity	30
5.2	Product density	36
5.3	Conditional intensity (temporal)	39
6	Discussion	41
	References	43

1 Introduction

Operational decisions in industry or the public sector often rely on forecasts of uncertain future quantities, in order to be informed on the likely implications of different actions. For example, quantitative criminology considers forecasts of increased criminal offenses ([Mohler et al., 2011](#); [Flaxman et al., 2019](#)), epidemiology studies when and where people catch diseases ([Meyer and Held, 2014](#); [Schoenberg et al., 2019](#)), and fire departments monitor the sources and areas of wildfires ([Peng et al., 2005](#); [Xu and Schoenberg, 2011](#); [Taylor et al., 2013](#)). The relevant events in these examples (criminal offenses, infections, wildfires) occur as random point patterns in space and time. In statistical terms they are point processes.

Beyond the development of new point process models for these phenomena, a growing interest centers around sound methods for the evaluation of forecasts and models. Many approaches to this problem are discussed in the context of seismology, where occurrences of earthquakes are interpreted as point processes and models are used to forecast statistical properties of seismic activity. Common methods to study the performance of these models include summary statistics such as the (weighted) K-function or receiver operating characteristic (ROC) curves and point process residuals, see e.g. [Bray and Schoenberg \(2013\)](#) for a review. Most notably, the regional earthquake likelihood models (RELM) initiative ([Field, 2007](#); [Schorlemmer et al., 2007](#)) developed various statistical tests to compare point process models for earthquake occurrence. To avoid bias, its testing centers perform fully prospective evaluation, i.e. they use only data recorded after model submission. Some of the employed tests connect to forecast evaluation via *proper scoring rules* ([Bray and Schoenberg, 2013](#)).

Consistent scoring functions and proper scoring rules are widely used and well-studied tools to assess relative performance, i.e. check whether one model or forecaster outperforms a competitor ([Gneiting and Raftery, 2007](#); [Gneiting, 2011](#)). Both are based on the principle of assigning a score or loss $S(a, y)$ to each pair of forecast or model output a and realized observation y of a random variable Y . If the forecast is a statistical property of Y , e.g. the mean or a quantile, this mapping is usually called scoring function,

whereas the term scoring rule is common when the forecasts are probabilistic, i.e. an entire distribution is reported. In both settings, the key requirement is that forecasting the truth gives the best score in expectation; a scoring function is *consistent* for a statistical property if the value of this property for a distribution F is a minimizer of the expected score with respect to F . Likewise, a scoring rule is *proper* if the expected score with respect to F is minimized by F . Apart from forecast comparison, propriety and consistency allow for regression and M-estimation (Gneiting and Raftery, 2007; Gneiting, 2011; Fissler and Ziegel, 2016) and can be used for statistical learning (Steinwart et al., 2014; Frongillo and Kash, 2021).

In this work we show that consistent scoring functions naturally transfer to the point process setting, which allows for decision-theoretically justified forecast evaluation and model comparison. This general connection unifies many existing methods, complements recent work by Heinrich et al. (2019), and paves the way for substantial improvements in forecast evaluation and model selection for point processes.

The manuscript is structured as follows. Section 2 recalls results on scoring functions, explains how they can be used in forecast evaluation or model selection, and sketches how to extend this to point processes. Section 3 rigorously introduces scoring functions for point patterns and considers consistency for various popular point process characteristics. Section 4 explains how some of the introduced scoring functions relate to existing methods of model assessment and Section 5 reports simulation results that illustrate the performance of the corresponding forecast evaluation methods. Section 6 concludes with an outlook towards further refinements and a discussion.

2 Scoring functions and forecast evaluation

This section starts with a short introduction on consistent scoring functions and then discusses how they can be used for comparative evaluation of forecasts or models. The overview and notation follow Gneiting (2011).

2.1 Preliminaries on scoring functions

Let \mathcal{O} and \mathcal{A} be subsets of a real vector space, called *observation domain* and *action domain*, respectively, and let \mathcal{F} be a collection of probability distributions on the Borel- σ -algebra of \mathcal{O} . We interpret $x \in \mathcal{A}$ as a forecast of a *functional* $T : \mathcal{F} \rightarrow \mathcal{A}$ of some random element in \mathcal{O} . A function $S : \mathcal{A} \times \mathcal{O} \rightarrow \mathbb{R}$ is called *scoring function* if for all $x \in \mathcal{A}$ the mapping $S(x, \cdot)$ is F -integrable for all $F \in \mathcal{F}$. The literature usually distinguishes point forecasts ($\mathcal{A} \subseteq \mathbb{R}^n$) and probabilistic forecasts ($\mathcal{A} = \mathcal{F}$ and T is the identity) and uses the term *scoring rule* in the probabilistic setting. We will not make this distinction and exclusively use the term scoring function.

The key idea motivating the use of scoring functions is *consistency*, meaning that a perfect forecast should achieve the lowest score in expectation. More precisely, we say that a scoring function S is *consistent* for a functional $T : \mathcal{F} \rightarrow \mathcal{A}$ if for all $x \in \mathcal{A}$ and

Table 1: Examples of pairs S and T , where the scoring function S is strictly consistent for the property T under appropriate conditions on \mathcal{F} . We identify a distribution $F \in \mathcal{F}$ with its cumulative distribution function $x \mapsto F((-\infty, x])$ and denote both by F

Action dom. \mathbf{A}	Observ. dom. \mathbf{O}	Property $T : \mathcal{F} \rightarrow \mathbf{A}$	Scoring function $S(x, y)$ or $S(F, y)$
$x \in \mathbb{R}$	$y \in \mathbb{R}$	mean	$(x - y)^2$
$x \in \mathbb{R}$	$y \in \mathbb{R}$	n -th moment	$-x^2 - 2x(y^n - x)$
$x \in \mathbb{R}$	$y \in \mathbb{R}$	τ -quantile	$(\mathbb{1}(y \leq x) - \tau)(x - y)$
$x \in \mathbb{R}$	$y \in \mathbb{R}$	τ -expectile	$ \mathbb{1}(y \leq x) - \tau (x - y)^2$
$F \in \mathcal{F}$	$y \in \mathbb{R}$	probab. density fct.	$-\log(F'(y))$
$F \in \mathcal{F}$	$y \in \mathbb{R}$	cumul. distrib. fct.	$\int_{-\infty}^{\infty} (F(x) - \mathbb{1}(y \leq x))^2 dx$

$F \in \mathcal{F}$ we have

$$\int_{\mathbf{O}} S(x, y) dF(y) \geq \int_{\mathbf{O}} S(T(F), y) dF(y), \quad (1)$$

or, reformulated in terms of a random variable Y with distribution F ,

$$\mathbb{E}_F S(x, Y) \geq \mathbb{E}_F S(T(F), Y).$$

It is *strictly consistent* for T if in addition equality in (1) implies $x = T(F)$. A central question is which functionals T are *elicitable*, i.e. possess a strictly consistent scoring function. Both concepts, elicibility and strict consistency, can thus be understood to refer to the same property of the pair S and T . Many elicitable functionals and the corresponding classes of strictly consistent scoring functions are known, see for instance [Gneiting and Raftery \(2007\)](#), [Gneiting \(2011\)](#), [Dawid and Musio \(2014\)](#), [Frongillo and Kash \(2015\)](#), and [Frongillo and Kash \(2021\)](#). Table 1 lists some prominent examples in the case $\mathbf{O} = \mathbb{R}$. In the situation $\mathbf{A} = \mathcal{F}$ the identity and restrictions to the tails are the most relevant functionals, see [Gneiting and Raftery \(2007\)](#), [Gneiting and Ranjan \(2011\)](#), [Lerch et al. \(2017\)](#), and [Holzmann and Klar \(2017\)](#).

A general result is that expectations of integrable functionals are always elicitable. To make this precise, let $\mathbf{A}, \mathbf{O} \subseteq \mathbb{R}^k$ and denote the subderivative of a convex function $f : \mathbf{A} \rightarrow \mathbb{R}^k$ at $x \in \mathbb{R}^k$ by $\nabla f(x)$. Then the function

$$b : \mathbf{A} \times \mathbf{O} \rightarrow \mathbb{R}, \quad (x, y) \mapsto -f(x) - \nabla f(x)^\top (y - x) \quad (2)$$

is called a *Bregman function* for f . If f is strictly convex, b is called *strictly consistent*. Using these definitions we can formulate the following result, see [Savage \(1971\)](#), [Gneiting \(2011\)](#), and [Frongillo and Kash \(2015\)](#).

Theorem 2.1 (Elicitability of expectations). *Let $h : \mathbf{O} \rightarrow \mathbb{R}^k$ be F -integrable for all $F \in \mathcal{F}$. Then the functional*

$$T : \mathcal{F} \rightarrow \mathbf{A} \subseteq \mathbb{R}^k, \quad T(F) = \int h(y) dF(y) = \mathbb{E}_F h(Y) = (\mathbb{E}_F h_1(Y), \dots, \mathbb{E}_F h_k(Y))^\top$$

is elicitable and consistent scoring functions $S : \mathbf{A} \times \mathbf{O} \rightarrow \mathbb{R}$ are given by $S(x, y) = b(x, h(y))$, where b is a Bregman function. If b is strictly consistent, then S is strictly consistent for T .

The next two results show how elicibility and consistency are compatible with transformations of the action or observation domain. In general, bijective mappings ensure elicibility, see [Gneiting \(2011, Theorem 4\)](#).

Proposition 2.2 (Revelation principle). *Let \mathbf{A}, \mathbf{A}' be some sets and $g : \mathbf{A} \rightarrow \mathbf{A}'$ a bijection with inverse g^{-1} . Let $T : \mathcal{F} \rightarrow \mathbf{A}$ and $T_g : \mathcal{F} \rightarrow \mathbf{A}'$ defined via $T_g(F) := g(T(F))$ be functionals. Then T is elicitable if and only if T_g is elicitable. A function $S : \mathbf{A} \times \mathbf{O} \rightarrow \mathbb{R}$ is a strictly \mathcal{F} -consistent scoring function for T if and only if $S_g : \mathbf{A}' \times \mathbf{O} \rightarrow \mathbb{R}$, $(x, y) \mapsto S_g(x, y) := S(g^{-1}(x), y)$ is a strictly \mathcal{F} -consistent scoring function for T_g .*

Example 2.3 (Variance). Although the variance functional $T_{\text{var}}(F) = \mathbb{E}_F Y^2 - (\mathbb{E}_F Y)^2$ fails to be elicitable ([Gneiting, 2011](#)), it is *jointly* elicitable with the mean: Define the functional $T : \mathcal{F} \rightarrow \mathbb{R}^2$ via $T(F) = (\mathbb{E}_F Y, T_{\text{var}}(F))^{\top}$ and observe that there exists a bijection between T and the functional T' given by $T'(F) = (\mathbb{E}_F Y, \mathbb{E}_F Y^2)^{\top}$. Since T' is elicitable by Theorem 2.1, elicibility of T follows from Proposition 2.2.

Analogous to changes of the action domain, the next result illustrates a straightforward connection between consistency and the observation domain. It resembles the findings on weighted functionals as discussed in [Gneiting and Ranjan \(2011\)](#) and [Gneiting \(2011, Theorem 5\)](#).

Proposition 2.4 (Transformation principle). *Let $g : \mathbf{O}' \rightarrow \mathbf{O}$ be a measurable mapping and \mathcal{F}' a set of distributions on \mathbf{O}' and define $g(\mathcal{F}') := \{F \circ g^{-1} \mid F \in \mathcal{F}'\}$. If there is an elicitable functional $T : g(\mathcal{F}') \rightarrow \mathbf{A}$, then the functional T' defined via $T'(F) := T(F \circ g^{-1})$ is elicitable and (strictly) consistent scoring functions for T' are given by $S'(x, y) = S(x, g(y))$, where S is a (strictly) consistent scoring function for T .*

2.2 Forecast comparison and score differences

Consistent scoring functions are useful statistical tools to address the question of relative performance when more than one forecast is available. If the forecasts are reports for an elicitable functional, then the previous subsection suggests a natural way of comparing their quality: Choose a strictly consistent scoring function for this functional and call a forecast superior to its competitor if it achieves a lower expected score. This allows for a choice between two forecasts based on their difference in expected scores, without further assumptions on the data-generating process. Although we focus on forecasting in the following, the principle is not restricted to such an application.

When using scoring functions in practice we have to rely on estimates, as the true expected score differences are not available. This motivates an intuitive forecast comparison setting, see e.g. [Nolde and Ziegel \(2017\)](#). Let $T : \mathcal{F} \rightarrow \mathbf{A}$ be an elicitable functional with strictly consistent scoring function $S : \mathbf{A} \times \mathbf{O} \rightarrow \mathbb{R}$ and consider a sequence of random variables $(Y_t)_{t \in \mathbb{N}}$ adapted to a filtration $(\mathcal{H}_t)_{t \in \mathbb{N}}$. Assume that forecasts of the

functional T applied to the conditional distribution $Y_t \mid \mathcal{H}_{t-1}$ are given. These forecasts can be regarded as random sequences $R = (R_t)_{t \in \mathbb{N}}$ and $R^* = (R_t^*)_{t \in \mathbb{N}}$ and their performance can be compared via the *average score difference*

$$\Delta_n(R, R^*) := \frac{1}{n} \sum_{t=1}^n S(R_t, Y_t) - \frac{1}{n} \sum_{t=1}^n S(R_t^*, Y_t) = \frac{1}{n} \sum_{t=1}^n (S(R_t, Y_t) - S(R_t^*, Y_t)), \quad (3)$$

which is an intuitive estimator for the difference in expected scores. Based on the law of large numbers and the strict consistency of S , a positive value supports the conjecture that R^* is superior to R , while a negative value supports the opposite conjecture.

A key issue which remains is assessing whether the size of the observed average score difference provides enough evidence to favor one of the two forecast sequences. The Diebold-Mariano (DM) test (Diebold and Mariano, 1995) addresses this aspect by testing whether $\Delta_n(R, R^*)$ is significantly different from zero. In the simple situation of an i.i.d. sequence $(Y_t)_{t \in \mathbb{N}}$, the forecast sequences reduce to constants $r, r^* \in \mathbf{A}$ and we can perform such a test based on the asymptotic normality of the well-known t-statistic $t_n := \sqrt{n} \Delta_n(r, r^*) / \sqrt{\hat{\sigma}_n^2}$, where $\hat{\sigma}_n^2$ estimates the variance of $S(r, Y) - S(r^*, Y)$. For more general time series $(Y_t)_{t \in \mathbb{N}}$, $(R_t)_{t \in \mathbb{N}}$, and $(R_t^*)_{t \in \mathbb{N}}$ we refer to the evaluation setting worked out in Nolde and Ziegel (2017), where tests for equal forecast performance rely on suitable asymptotic results developed in Giacomini and White (2006).

2.3 Application to point process settings

The previous subsections introduce the concepts of consistency and elicibility for distributions of some generic random variable Y and a functional T . The central objective of this manuscript is to show that both ideas and the related statistical methods can be transferred to the point process setting. This gives valuable tools for comparative forecast evaluation of a variety of statistical properties for point processes (see Section 3 for examples). For clarity of presentation, we distinguish three different point process scenarios, based on common applications:

Scenario A (purely spatial) In this scenario the process is defined on either a single domain (Scenario A1), or non-overlapping subdomains with no (or little) dependence between them (Scenario A2). Examples include the points which an observer fixates in an image (Barthelmé et al., 2013) or the locations of trees in a forest (Stoyan and Penttinen, 2000). Stationarity is a common simplifying assumption in this context.

Scenario B (purely temporal) In this scenario, there is no spatial component and the process consists of points in time only. Examples are the arrival times of e-mails (Fox et al., 2016) or times of infections with a disease (Schoenberg et al., 2019). In this special setting the directional character of time allows for a distinct interpretation and treatment.

Scenario C (spatio-temporal) Additional to the spatial component, processes in this scenario possess a temporal component, which could be discrete (Scenario C1)

or continuous (Scenario C2). Examples are locations of crime hotspots in a city (Mohler et al., 2011) or earthquakes over time in a specific region (Ogata, 1998; Zhuang et al., 2002).

In order to compare forecasts in each of these scenarios, the ideas of the previous subsection can be used as follows. Let Φ be a point process and S a scoring function such that $S(a, \Phi)$ is the score of the report $a \in \mathbf{A}$. Moreover, assume that S is strictly consistent for a statistical property of point processes e.g. the intensity. Section 3 discusses which other properties and scoring functions are available, as well as technical details. In this situation two forecasts a and a^* can be compared based on the sign of the expectation $\mathbb{E}[S(a, \Phi) - S(a^*, \Phi)]$, where, due to the consistency of S , negative values support a , while positive values support a^* .

Given point process realizations Φ_1, \dots, Φ_n the difference in expected scores can be accessed via the average score difference as in (3). Although the idea of score differences is the same for all three scenarios, the detailed estimation may vary among them. In particular, as discussed in Subsection 2.2, it is desirable in applications to estimate the uncertainty inherent in the average score differences. Due to the more complex structure of point processes this task depends on whether the process has a continuous or a discrete time component.

Discrete time Assume that the point process data is sampled at fixed points in time, i.e. it can be modeled by a sequence $(\Phi_t)_{t \in \mathbb{N}}$ adapted to a filtration $(\mathcal{H}_t)_{t \in \mathbb{N}}$. This setting includes the special case of i.i.d. realizations and relates to Scenario C1 as well as variants of Scenario A. Since the score differences $(S(R_t, \Phi_t) - S(R_t^*, \Phi_t))_{t \in \mathbb{N}}$ form a sequence of real-valued random variables, the ideas of Subsection 2.2, particularly the comparative testing framework of Nolde and Ziegel (2017) and its asymptotic results, are directly applicable. This yields an approach to forecasts evaluation and model selection which is suitable if dependence does not exist or is not of central interest for evaluation.

Continuous time If we consider point processes in Scenario C2 or Scenario B, then temporal dependence between the points of Φ becomes an essential feature of the process and can also be object of the forecast. Apart from that, it has to be accounted for in estimation and testing, since it will affect asymptotic results. To see this, assume for simplicity that Φ is a purely temporal process observed over a time period $[0, T]$ with $0 < t_1 < \dots < t_k < T$ denoting the corresponding arrival times. In a stepwise forecast setting, where the reports R_i and R_i^* can adapt to previous arrivals t_1, \dots, t_{i-1} (see e.g. Subsection 3.5), this yields a realized score difference

$$\Delta_T(R, R^*) = \sum_{i=1}^{n(T)} (S(R_i, t_i) - S(R_i^*, t_i)), \quad (4)$$

where $n(T) := \Phi([0, T])$ is the random number of points in $[0, T]$. In contrast to (3) we do not consider averages since dividing by $n(T)$ will interfere with the consistency of S . The

score difference $\Delta_T(R, R^*)$ is a sum of a random number of random variables, usually called a random sum. This perspective connects the estimation of score differences to the theory of total claim amount in insurance, see e.g. Mikosch (2009) and Embrechts et al. (1997).

Asymptotic results for the score difference (4) for $T \rightarrow \infty$ are desirable to assess the uncertainty of the forecast evaluation task. One possible approach to this problem relies on limit theorems for randomly indexed processes due to Anscombe (1952), in particular random central limit theorems: If the number of points $n(T)$ satisfies a weak law of large numbers, then under Anscombe's condition, we only have to ensure that the sequence $(S(R_i, t_i) - S(R_i^*, t_i))_{i \in \mathbb{N}}$ satisfies a central limit theorem in order to obtain asymptotic normality for (4). Such results are available for strong mixing (Lee, 1997), ψ -weakly dependent (Hwang and Shin, 2012), and m -dependent (Shang, 2012) sequences, but a detailed discussion is beyond the scope of this manuscript.

3 Consistent scoring functions for point patterns

This section explores which consistent scoring functions are available if the observations are finite point patterns in a set $\mathcal{X} \subseteq \mathbb{R}^d$. We start with general principles which connect to existing theory (Subsection 2.1) and then derive scoring functions for a variety of popular point process properties, which relate to Scenario A, B, and C of Subsection 2.3.

3.1 Technical context

A finite *point process* Φ is a random element in the space $\mathbb{M}_0 = \mathbb{M}_0(\mathcal{X})$ of finite counting measures on \mathcal{X} , cf. Daley and Vere-Jones (2003) for details. Hence, our observation domain is \mathbb{M}_0 in this context and we shall denote a set of probability measures on \mathbb{M}_0 by \mathcal{P} and the distribution of Φ by P_Φ . As in Subsection 2.1, a *functional* is a mapping $\Gamma : \mathcal{P} \rightarrow \mathbb{A}$, where \mathbb{A} is an action domain, and we call a mapping $S : \mathbb{A} \times \mathbb{M}_0 \rightarrow \mathbb{R}$ a *scoring function* if $\mathbb{E}_P S(a, \Phi) = \int S(a, \varphi) dP(\varphi)$ exists for all $a \in \mathbb{A}$ and $P \in \mathcal{P}$. *Elicitability* of Γ as well as (*strict*) *consistency* of S is then defined as above via inequality (1).

For ease of presentation and practical implementation, we will usually state how the score of a realization $\varphi = \sum_{i=1, \dots, n} \delta_{y_i} \in \mathbb{M}_0$ is computed from an enumeration of its points, i.e. from the set $\{y_1, \dots, y_n\}$ if $n = |\varphi|$. For $n = 0$ no points occurred, so the set is empty. To make this meaningful, we will ensure that for spatial processes all scoring functions are independent of the enumeration of points (see also Daley and Vere-Jones (2003, Section 5.3)). For temporal processes we use the natural enumeration which orders the points from smallest to largest.

In light of the results of Subsection 2.1, constructing simple examples for elicitable functionals of point processes is straightforward: Since point processes induce real-valued random variables in many ways, the expectations of these random variables (provided they are well-defined) will be elicitable functionals.

Example 3.1 (Expected number of points). Given a set $B \in \mathcal{B}(\mathcal{X})$, the (\mathbb{N}_0 -valued) random variable $\Phi(B)$ denotes the random number of points of Φ in B . If the functional

$\Gamma_B : \mathcal{P} \rightarrow \mathbb{R}$ given by $\Gamma_B(P) = \mathbb{E}_P \Phi(B)$ is well-defined, Theorem 2.1 shows that it is elicitable with Bregman scoring function

$$S_B(x, \varphi) = b(x, \varphi(B)) = -f(x) - \nabla f(x)^\top (\varphi(B) - x),$$

where $f : [0, \infty) \rightarrow \mathbb{R}$ is a strictly convex function.

This construction is not limited to the expected number of points in a set, but works for any combination of elicitable functional (e.g. expectation) and point process feature (e.g. number of points). More precisely, let \mathcal{O} be an observation domain, $g : \mathbb{M}_0 \rightarrow \mathcal{O}$ a measurable mapping and $g(\mathcal{P}) := \{P \circ g^{-1} \mid P \in \mathcal{P}\}$. Due to the transformation principle (Proposition 2.4), the functional $\Gamma(P) := T(P \circ g^{-1})$ is elicitable whenever $T : g(\mathcal{P}) \rightarrow \mathbb{A}$ is elicitable. We recover Example 3.1 by choosing $T(F) = \mathbb{E}_F Y$ and $g(\varphi) = \varphi(B)$. The elicibility of other “simple” properties like finite-dimensional distributions and void probabilities is a straightforward consequence of Proposition 2.4.

Example 3.2 (Void probability). For any fixed set $B \in \mathcal{B}(\mathcal{X})$ the functional Γ defined via $\Gamma(P) = \mathbb{P}_P(\Phi(B) = 0)$ is elicitable.

Example 3.3 (Point process integrals). Fix some measurable functions $f_i : \mathcal{X} \rightarrow \mathbb{R}$, $i = 1, \dots, m$ for $m \in \mathbb{N}$. Define $g : \mathbb{M}_0 \rightarrow \mathbb{R}^m$ via

$$g(\varphi) = \left(\int_{\mathcal{X}} f_1 d\varphi, \dots, \int_{\mathcal{X}} f_m d\varphi \right)^\top = \left(\sum_{x_i \in \varphi} f_1(x_i), \dots, \sum_{x_i \in \varphi} f_m(x_i) \right)^\top$$

and let $T = \text{id}_{g(\mathcal{P})}$. Then the finite-dimensional distribution functional $\Gamma_{f_1, \dots, f_m}(P) = T(P \circ g^{-1})$ is an elicitable property of the point process Φ .

As illustrated by the previous examples, different choices for T and g in Proposition 2.4 lead to a wide variety of different functionals and consistent scoring functions. In Heinrich et al. (2019) the main idea is to choose T as the identity on $g(\mathcal{P})$ (see also Example 3.3). Two distributional models $P, Q \in \mathcal{P}$ of the process Φ can then be compared based on realizations by comparing $P \circ g^{-1}$ and $Q \circ g^{-1}$ via a consistent scoring function S . The mapping $g : \mathbb{M}_0 \rightarrow \mathcal{O}$ is selected to be an estimator of some quantity of interest, e.g. a kernel-based intensity estimator. Since the distributions of such estimators will usually not be explicitly available, approximating the scoring functions via simulations becomes necessary. Moreover, as different $P \in \mathcal{P}$ may lead to the same law $P \circ g^{-1}$, this approach hinges on the ability of g to discriminate between two distributions P and Q .

Instead of following this approach and using Proposition 2.4, we focus on common point process characteristics $\Gamma : \mathcal{P} \rightarrow \mathbb{A}$ and develop strictly consistent scoring functions for them. Important examples for Γ include the point process distribution and the intensity measure. This allows for a direct comparison of the characteristic Γ , which includes distributional models $P \in \mathcal{P}$ as a special case. In contrast, comparison in Heinrich et al. (2019) always depends on specific aspects of the distributions in \mathcal{P} which are determined via the ‘estimator choice’ g . The discrimination ability of our approach depends on how

similar the property values $\Gamma(P)$ and $\Gamma(Q)$ (e.g. the intensity measures) are. In particular, knowledge of the distribution P is not needed as long as $\Gamma(P)$ is available. In cases where Γ can be computed explicitly, this avoids possibly high computational costs owing to point process simulations.

3.2 Density and distribution – general processes

This subsection constructs consistent scoring functions for the whole distribution P_Φ of the finite point process Φ , which corresponds to the identity functional $\Gamma = \text{id}_P$. We obtain two results, corresponding to distinct representations of the distribution P_Φ . Although applicable to general processes, the main focus is Scenario A and related results for temporal point processes are given in Subsection 3.5.

For our first approach we use the fact that the law P_Φ of a finite point process on \mathcal{X} can be equivalently represented by two sequences $(\Pi_k)_{k \in \mathbb{N}}$ and $(p_k)_{k \in \mathbb{N}_0}$. Each p_k specifies the probability of finding k points in a realization. The Π_k are symmetric probability measures on \mathcal{X}^k which describe the distribution of any ordering of points, given k points are realized, see Daley and Vere-Jones (2003, Chapter 5.3) for details. We can thus construct scoring functions for the distribution of the process by combining scoring functions for all Π_k with a scoring function for the distribution $(p_k)_{k \in \mathbb{N}_0}$.

To state this result, we introduce the notion of *symmetric* scoring functions, where $S : \mathbf{A} \times \mathbb{R}^n \rightarrow \mathbb{R}$ is called symmetric if $S(a, y_1, \dots, y_n) = S(a, y_{\pi(1)}, \dots, y_{\pi(n)})$ holds for all $a \in \mathbf{A}$, $y \in \mathbb{R}^n$ and permutations π . Via this definition we ensure that the scoring functions of this subsection are independent of the enumeration of the realization of Φ .

Proposition 3.4. *Let \mathcal{P} be a class of distributions of finite point processes, with $Q \in \mathcal{P}$ decomposed into $(\Pi_k^Q)_{k \in \mathbb{N}}$ and $(p_k^Q)_{k \in \mathbb{N}_0}$. Set $\mathcal{F}_k := \{\Pi_k^Q \mid Q \in \mathcal{P}\}$ and let $S_k : \mathcal{F}_k \times \mathcal{X}^k \rightarrow \mathbb{R}$ be a symmetric (strictly) consistent scoring function for $\text{id}_{\mathcal{F}_k}$ for all $k \in \mathbb{N}$. Let S_0 be a (strictly) consistent scoring function for distributions on \mathbb{N}_0 . Then the function $S : \mathcal{P} \times \mathbb{M}_0 \rightarrow \mathbb{R}$ defined via*

$$S(((\Pi_k^Q)_{k \in \mathbb{N}}, (p_k^Q)_{k \in \mathbb{N}_0}), \{y_1, \dots, y_n\}) = S_n(\Pi_n^Q, y_1, \dots, y_n) + S_0((p_k^Q)_{k \in \mathbb{N}_0}, n)$$

for $n \in \mathbb{N}$ and $S(((\Pi_k^Q)_{k \in \mathbb{N}}, (p_k^Q)_{k \in \mathbb{N}_0}), \emptyset) := S_0((p_k^Q)_{k \in \mathbb{N}_0}, 0)$ is a consistent scoring function for the distribution of the point process Φ . It is strictly consistent if S_0 and $(S_k)_{k \in \mathbb{N}}$ are strictly consistent.

Proof. The result follows by decomposing the expectation $\mathbb{E}_P S(Q, \Phi)$ into expectations on the sets $\{\Phi = n\}$ for $n \in \mathbb{N}$ and using the (strict) consistency of S_n on each set. \square

Although Proposition 3.4 allows for a general choice of scoring functions for the distributions $(\Pi_k)_{k \in \mathbb{N}}$, probability densities are often more convenient vehicles, especially when multivariate distributions are of interest. Gneiting and Raftery (2007) assume a measurable space (Ω, \mathcal{A}) with a σ -finite measure μ . They define the classes \mathcal{L}_α for $\alpha > 1$ which contain all densities p of probability measures P that are absolutely continuous

with respect to μ and such that

$$\|p\|_\alpha := \left(\int_{\Omega} p(\omega)^\alpha d\mu(\omega) \right)^{1/\alpha}$$

is finite. In this setting, important examples of strictly consistent scoring functions $S : \mathcal{L}_\alpha \times \Omega \rightarrow \mathbb{R}$ are the *pseudospherical* and the *logarithmic* score, defined via

$$\text{PseudoS}(p, \omega) = -p(\omega)^{\alpha-1} / \|p\|_\alpha^{\alpha-1} \quad \text{and} \quad \text{LogS}(p, \omega) = -\log p(\omega), \quad (5)$$

respectively. The logarithmic score is the (appropriately scaled) limiting case of the pseudospherical score for $\alpha \rightarrow 1$, see [Gneiting and Raftery \(2007\)](#) for details.

Returning to point processes we follow [Daley and Vere-Jones \(2003\)](#) and let P_0 denote the distribution of the Poisson point process with unit rate on some bounded domain $\mathcal{X} \subset \mathbb{R}^d$. If $P \in \mathcal{P}$ is absolutely continuous with respect to P_0 , then the Radon-Nikodým density dP/dP_0 exists and can be regarded as the density of P . It can be computed via the identity $dP/dP_0(\varphi) = \exp(|\mathcal{X}|)j_k(y_1, \dots, y_k)/k!$, where $|\mathcal{X}|$ denotes the Lebesgue measure of \mathcal{X} , y_1, \dots, y_k are the points of $\varphi \in \mathbb{M}_0$ and the (symmetric) function j_k defined via

$$j_k(x_1, \dots, x_k) dx_1 \cdots dx_k = k! p_k d\Pi_k(x_1, \dots, x_k) \quad (6)$$

is the so-called *k*-th *Janossy density* of Φ . For $k = 0$ this is interpreted as $j_0 = p_0$. The value $j_k(x_1, \dots, x_k)$ can be understood as the *likelihood* of k points materializing, one of them in each of the distinct locations $x_1, \dots, x_k \in \mathcal{X}$. We refer to [Daley and Vere-Jones \(2003, Chapter 7.1 and 5.3\)](#) for further details.

In principle, the previous discussion and (5) allow us to obtain scoring functions for the point process distribution P based on its densities $(j_k^P)_{k \in \mathbb{N}_0}$. However, two important difficulties have to be addressed in the point process setting. Firstly, explicit expressions for $(j_k)_{k \in \mathbb{N}_0}$ are usually hard to determine and known only for some models, see [Daley and Vere-Jones \(2003, Chapter 7.1\)](#) and Examples 3.5 and 3.6 below. Secondly, even if explicit expressions are available, calculating the norm $\|dP/dP_0\|_\alpha$ amounts to computing $(k!)^{-1} \int j_k(x_1, \dots, x_k)^\alpha dx_1 \cdots dx_k$ for all $k \in \mathbb{N}$, which may be prohibitive. This complicates the use of scoring functions relying on $\|\cdot\|_\alpha$, e.g. the pseudospherical score, see (5). We will thus only discuss two choices of scoring functions, the logarithmic and the Hyvärinen score.

Logarithmic score Assume that for all distributions $Q \in \mathcal{P}$ the Janossy densities $(j_k^Q)_{k \in \mathbb{N}_0}$ are well-defined. Due to the strict consistency of the logarithmic score ([Gneiting and Raftery, 2007](#)), the function $S : \mathcal{P} \times \mathbb{M}_0 \rightarrow \mathbb{R}$ defined via

$$S((j_k^Q)_{k \in \mathbb{N}_0}, \{y_1, \dots, y_n\}) = -\log(j_n^Q(y_1, \dots, y_n)) \quad (7)$$

for $n \in \mathbb{N}$ and $S((j_k^Q)_{k \in \mathbb{N}_0}, \emptyset) := -\log(j_0^Q)$ is a strictly consistent scoring function for the distribution of the point process Φ . The term $-|\mathcal{X}| + \log(n!)$ can be omitted, since it is independent of the report $(j_k^Q)_{k \in \mathbb{N}_0}$. This choice recovers the log-likelihood of the point process distribution Q from the perspective of consistent scoring functions.

Example 3.5 (Poisson point process). Let Φ be an inhomogeneous Poisson point process with intensity $\lambda : \mathcal{X} \rightarrow [0, \infty)$. It is well-known that Φ admits the densities

$$j_{n,\lambda}(y_1, \dots, y_n) = \left(\prod_{i=1}^n \lambda(y_i) \right) \exp \left(- \int_{\mathcal{X}} \lambda(y) \, dy \right)$$

for $n \in \mathbb{N}$, see e.g. [Daley and Vere-Jones \(2003, Chapter 7\)](#). In case $n = 0$ the product is interpreted as one. When reporting the Poisson point process distribution P_Φ via its Janossy densities, [\(7\)](#) gives the score

$$S(P_\Phi, \{y_1, \dots, y_n\}) = - \sum_{i=1}^n \log \lambda(y_i) + \int_{\mathcal{X}} \lambda(y) \, dy \quad (8)$$

for $n \in \mathbb{N}$ and $S(P_\Phi, \emptyset) = |\lambda|$, where $|\lambda| = \int_{\mathcal{X}} \lambda(y) \, dy$. In the context of [Proposition 3.4](#), the definition of Poisson point processes implies that the distribution of Φ can be decomposed via

$$d\Pi_n(y_1, \dots, y_n) = \prod_{i=1}^n \frac{\lambda(y_i)}{|\lambda|} \, dy_1 \cdots dy_n \quad \text{and} \quad p_n = \frac{|\lambda|^n}{n!} e^{-|\lambda|}.$$

When choosing all the scoring functions $(S_n)_{n \in \mathbb{N}}$ and S_0 as the logarithmic score the scoring function S in [Proposition 3.4](#) simplifies and agrees with [\(8\)](#).

The previous example illustrates how the scoring functions for $(\Pi_k, p_k)_{k \in \mathbb{N}_0}$ and $(j_k)_{k \in \mathbb{N}_0}$ are connected in the case of Poisson point processes. In general, identity [\(6\)](#) shows that choosing the logarithmic score for $(S_n)_{n \in \mathbb{N}}$ and S_0 leads to identical scoring functions in [\(7\)](#) and [Proposition 3.4](#). For other choices, relating both expressions is an open problem.

Hyvärinen score Apart from the Poisson point process, some other models admit explicit expressions for $(j_k)_{k \in \mathbb{N}_0}$ or the densities of $(\Pi_k)_{k \in \mathbb{N}}$, however, often only up to unknown normalizing constants. In this situation, 0-homogeneous consistent scoring functions for densities can be of use, i.e. S which satisfy $S(cf, y) = S(f, y)$ for all $c > 0$. This property allows for the consistent evaluation of a density without the normalizing constant being known. The most relevant scoring function of this type is the *Hyvärinen score* defined via

$$\text{HyvS}(f, y) := \Delta \log f(y) + \frac{1}{2} \|\nabla \log f(y)\|^2,$$

where ∇ denotes the gradient, Δ is the Laplace operator, and f is a twice differentiable density on \mathbb{R}^d . To ensure strict consistency on a class of probability densities \mathcal{L} its members have to be positive almost everywhere and for all $f, g \in \mathcal{L}$ it must hold that $\nabla \log(f(y))g(y) \rightarrow 0$ as $\|y\| \rightarrow \infty$, see [Hyvärinen \(2005\)](#), [Dawid et al. \(2012\)](#), and [Ehm and Gneiting \(2012\)](#) for details.

Similar to the logarithmic score, we can transfer the Hyvärinen score to the point process setting. To do this we assume that for all $Q \in \mathcal{P}$ and $k \in \mathbb{N}$, j_k^Q is defined on $(\mathbb{R}^d)^k$ and satisfies the regularity conditions of the Hyvärinen score. Then the function $S : \mathcal{P} \times \mathbb{M}_0 \rightarrow \mathbb{R}$ defined via

$$S((j_k^Q)_{k \in \mathbb{N}_0}, \{y_1, \dots, y_n\}) = -\text{HyvS}(j_n^Q, y_1, \dots, y_n) \quad (9)$$

for $n \in \mathbb{N}$ and $S((j_k^Q)_{k \in \mathbb{N}_0}, \emptyset) := 0$ is a consistent scoring function for the distribution of the point process Φ . Observe that we cannot achieve strict consistency for S , since the probability of $|\Phi| = n$ is proportional to j_n (see identity (6)) and thus not accessible to the Hyvärinen score.

Example 3.6 (Gibbs point process). Stemming from theoretical physics, Gibbs processes are a popular tool to model particle interactions. They are defined via their Janossy densities

$$j_n(y_1, \dots, y_n) = C(\theta) \exp(-\theta U(y_1, \dots, y_n)),$$

where U represents the point interactions, θ is a parameter relating to the temperature, and C is the partition function, which ensures that the collection $(j_k)_{k \in \mathbb{N}_0}$ is properly normalized, see e.g. Daley and Vere-Jones (2003, Chapter 5.3) and Chiu et al. (2013, Chapter 5.5). It is in general difficult to find expressions for C or even approximate it, hence the Hyvärinen score might seem attractive to evaluate models based on $(j_k)_{k \in \mathbb{N}_0}$. Plugging j_n into (9) gives

$$S((j_k)_{k \in \mathbb{N}_0}, \{y_1, \dots, y_n\}) = \theta \left[-\Delta U(y_1, \dots, y_n) + \frac{\theta}{2} \|\nabla U(y_1, \dots, y_n)\|^2 \right]$$

for $n \in \mathbb{N}$, where the derivatives are computed with respect to the coordinates of the vector $(y_1, \dots, y_n) \in (\mathbb{R}^d)^n$. The simplest choice for interactions is to restrict U to first- and second-order terms

$$U(y_1, \dots, y_n) := \sum_{i=1}^n l(y_i) + \sum_{i,j=1}^n \psi(\|y_i - y_j\|^2)$$

for $l : \mathbb{R}^d \rightarrow \mathbb{R}$ and $\psi : [0, \infty) \rightarrow [0, \infty)$ with $\psi(0) = 0$, see e.g. Daley and Vere-Jones (2003, Chapter 5.3). To apply the Hyvärinen score in this setting, l and ψ have to satisfy some regularity conditions detailed in Hyvärinen (2005), and in particular admit second order derivatives almost everywhere. The soft-core models for ψ introduced in Ogata and Tanemura (1984) satisfy this condition, while their hard-core model for ψ is not even continuous. An additional technical issue is that Ogata and Tanemura (1984) consider point processes on a finite domain \mathcal{X} and use a constant l . To make the Hyvärinen score applicable in this setting a possible solution is to approximate their models via twice differentiable densities on $(\mathbb{R}^d)^n$.

3.3 Intensity and moment measures

As one of the key characteristics of point processes, the intensity measure, or more general moment measures, can be interpreted as analogons to the moments of a univariate random variable. To construct scoring functions for these measures, let $\mathcal{X} \subset \mathbb{R}^d$ be bounded and $\mathcal{M}_f = \mathcal{M}_f(\mathcal{X})$ a set of finite measures on \mathcal{X} . We call $\Lambda^* := \Lambda/|\Lambda|$, where $|\Lambda| := \Lambda(\mathcal{X})$, the *normalized measure* of a finite measure $\Lambda \in \mathcal{M}_f$.

Intensity measure The intensity measure $\Lambda : B \mapsto \mathbb{E}\Phi(B)$ quantifies the expected number of points in a set $B \in \mathcal{B}(\mathcal{X})$, see e.g. [Daley and Vere-Jones \(2003\)](#) and [Chiu et al. \(2013\)](#). It is one of the central tools to describe average point process behavior and is thus essential in many applications in Scenario A or C. For a fixed Borel set B , the expected number of points was already discussed in Example 3.1, thus here we focus on scoring functions for the full measure. We begin by considering the normalized intensity measure, since it is a probability measure.

Proposition 3.7. *Set $\mathcal{F} := \{\Lambda^* \mid \Lambda \in \mathcal{M}_f\}$ and let $S' : \mathcal{F} \times \mathcal{X} \rightarrow \mathbb{R}$ be a (strictly) consistent scoring function for $\text{id}_{\mathcal{F}}$. The scoring function $S : \mathcal{F} \times \mathbb{M}_0 \rightarrow \mathbb{R}$ defined via*

$$S(\Lambda^*, \{y_1, \dots, y_n\}) := \sum_{i=1}^n S'(\Lambda^*, y_i)$$

for $n \in \mathbb{N}$ and $S(\Lambda^*, \emptyset) = 0$ is consistent for the normalized intensity measure. It is strictly consistent if S' is strictly consistent.

Proof. Let $Q \in \mathcal{M}_f$ and Φ be a point process with intensity measure $\Lambda \in \mathcal{M}_f$ and distribution $P_\Phi \in \mathcal{P}$. Using Campbell's theorem, the difference in expected scores is

$$\begin{aligned} \mathbb{E}S(Q^*, \Phi) - \mathbb{E}S(\Lambda^*, \Phi) &= \int \sum_{x \in \varphi} S'(Q^*, x) - S'(\Lambda^*, x) dP_\Phi(\varphi) \\ &= \int_{\mathcal{X}} S'(Q^*, x) - S'(\Lambda^*, x) d\Lambda(x) \\ &= |\Lambda| \int_{\mathcal{X}} S'(Q^*, x) - S'(\Lambda^*, x) d\Lambda^*(x) \geq 0, \end{aligned}$$

where the inequality follows from the consistency of S' . If the difference is zero and S' is strictly consistent, this gives $Q^* = \Lambda^*$, showing that S is strictly consistent for the normalized intensity measure. \square

In principle, it is possible to define scoring functions for non-normalized measures, as well. [Hendrickson and Buehler \(1971\)](#) use a constant extension of scoring functions to the cone induced by a set of probability measures, in order to connect to homogeneous convex functions. However, as the proof of Proposition 3.7 illustrates, information concerning the intensity measure can be accessed only after normalization. Since the total mass $|\Lambda| = \mathbb{E}\Phi(\mathcal{X})$ is an elicitable property of Φ (see Example 3.1), combining this information with Λ^* leads to a consistent scoring function for the (unnormalized) intensity. This follows from an application of the revelation principle (Proposition 2.2).

Corollary 3.8. Set $\mathcal{F} := \{\Lambda^* \mid \Lambda \in \mathcal{M}_f\}$ and let $S' : \mathcal{F} \times \mathcal{X} \rightarrow \mathbb{R}$ be a (strictly) consistent scoring function for $\text{id}_{\mathcal{F}}$. Let $b : [0, \infty) \times [0, \infty) \rightarrow \mathbb{R}$ be a (strictly) consistent Bregman function, as defined in (2). The scoring function $S : \mathcal{M}_f \times \mathbb{M}_0 \rightarrow \mathbb{R}$ defined via

$$S(\Lambda, \{y_1, \dots, y_n\}) := \sum_{i=1}^n S'(\Lambda^*, y_i) + cb(|\Lambda|, n)$$

for $n \in \mathbb{N}$ and $S(\Lambda, \emptyset) = cb(|\Lambda|, 0)$ for $c > 0$ is consistent for the intensity measure. It is strictly consistent if both S' and b are strictly consistent.

Example 3.9. As an important special case, assume that each $\Lambda \in \mathcal{M}_f$ admits a density λ with respect to Lebesgue measure. Using the common quadratic score for b and the logarithmic score (see (5)) for S' , the strictly consistent scoring function of Corollary 3.8 becomes

$$S(\Lambda, \{y_1, \dots, y_n\}) = - \sum_{i=1}^n \log(\lambda(y_i)) + n \log |\Lambda| + c(|\Lambda| - n)^2$$

for some $c > 0$. If we choose the logarithmic score for b and $c = 1$, then S leads to the same score as obtained in (8) for Poisson point process reports. This resembles the construction of the Dawid-Sebastiani score (Dawid and Sebastiani, 1999) and is further discussed in Section 4.3. Simulation experiments in Subsection 5.1 illustrate how S compares different intensity forecasts.

The choice of the constant $c > 0$ in Corollary 3.8 is irrelevant for (strict) consistency of the scoring function S . However, since S evaluates a mixture of shape and normalization of the intensity, where c balances the magnitudes of the scoring components, a careful choice will likely be crucial in applications.

Moment Measures When the intensity is interpreted as the first moment of a point process, moment measures generalize this notion to higher moments. Thereby, they are useful tools to quantify point interactions for processes occurring in Scenario A or C. Strictly consistent scoring functions for these measures can be constructed in the same way as for the intensity. For $n \in \mathbb{N}$, let $\mathcal{M}_f^n = \mathcal{M}_f(\mathcal{X}^n)$ be the set of finite Borel measures on \mathcal{X}^n . For positive measurable functions $f : \mathcal{X}^n \rightarrow (0, \infty)$ the n -th moment measure $\mu^{(n)}$ and the n -th factorial moment measure $\alpha^{(n)}$ are defined via the relations

$$\mathbb{E} \left[\sum_{x_1, \dots, x_n \in \Phi} f(x_1, \dots, x_n) \right] = \int_{\mathcal{X}^n} f(x_1, \dots, x_n) d\mu^{(n)}(x_1, \dots, x_n),$$

and

$$\mathbb{E} \left[\sum_{x_1, \dots, x_n \in \Phi}^{\neq} f(x_1, \dots, x_n) \right] = \int_{\mathcal{X}^n} f(x_1, \dots, x_n) d\alpha^{(n)}(x_1, \dots, x_n),$$

respectively, see e.g. Chiu et al. (2013) and Daley and Vere-Jones (2003). Here Σ^{\neq} denotes summation over all n -tuples that contain distinct points of Φ . Using the notion

of factorial product defined via

$$m^{[n]} := \begin{cases} m(m-1)(m-2)\cdots(m-n+1) & , m \geq n \\ 0 & , m < n \end{cases}$$

for $m, n \in \mathbb{N}$ we obtain the concise representations $\mu^{(n)}(B^n) = \mathbb{E}\Phi(B)^n$ and $\alpha^{(n)}(B^n) = \mathbb{E}\Phi(B)^{[n]}$ for Borel sets $B \in \mathcal{B}(\mathcal{X})$, see e.g. [Daley and Vere-Jones \(2003, Chapter 5\)](#). The next result follows by using the same arguments as in the proof of Proposition 3.7 together with the revelation principle (Proposition 2.2).

Proposition 3.10. *Set $\mathcal{F}^n := \{P^* \mid P \in \mathcal{M}_f^n\}$, let $S : \mathcal{F}^n \times \mathcal{X}^n \rightarrow \mathbb{R}$ be a (strictly) consistent scoring function for $\text{id}_{\mathcal{F}^n}$ and $b : [0, \infty) \times [0, \infty) \rightarrow \mathbb{R}$ a (strictly) consistent Bregman function.*

(i) *The function $S_1 : \mathcal{M}_f^n \times \mathbb{M}_0 \rightarrow \mathbb{R}$ defined via*

$$S_1(\mu, \{y_1, \dots, y_m\}) = \sum_{x_1, \dots, x_n \in \{y_1, \dots, y_m\}} S(\mu^*, x_1, \dots, x_n) + cb(\mu(\mathcal{X}^n), m^n)$$

for $m \in \mathbb{N}$ and $S_1(\mu, \emptyset) = cb(\mu(\mathcal{X}^n), 0)$ for $c > 0$ is a consistent scoring function for the n -th moment measure.

(ii) *The function $S_2 : \mathcal{M}_f^n \times \mathbb{M}_0 \rightarrow \mathbb{R}$ defined via*

$$S_2(\alpha, \{y_1, \dots, y_m\}) = \sum_{x_1, \dots, x_n \in \{y_1, \dots, y_m\}}^{\neq} S(\alpha^*, x_1, \dots, x_n) + cb(\alpha(\mathcal{X}^n), m^{[n]})$$

for $m \geq n$ and $S_2(\alpha, \{y_1, \dots, y_m\}) = cb(\alpha(\mathcal{X}^n), 0)$ for $m < n$ and with $c > 0$ is a consistent scoring function for the n -th factorial moment measure.

Both S_1 and S_2 are strictly consistent if S and b are strictly consistent.

In many cases of interest $\alpha^{(n)}$ is absolutely continuous with respect to Lebesgue measure on \mathcal{X}^n and its density $\varrho^{(n)}$ is called *product density*, see e.g. [Chiu et al. \(2013\)](#). A (strictly) consistent scoring function for $\varrho^{(n)}$ can be obtained from Proposition 3.10 (ii) by choosing S to be a strictly consistent scoring function for densities, as in the next example.

Example 3.11. Let $n = 2$ and for simplicity consider the product density $\varrho^{(2)}$ of a stationary and isotropic point process. In this situation, $\varrho^{(2)}$ depends on the point distances only, i.e. it can be represented via $\varrho^{(2)}(x_1, x_2) = \varrho_0^{(2)}(\|x_1 - x_2\|)$ for some $\varrho_0^{(2)} : [0, \infty) \rightarrow [0, \infty)$. Analogous to Example 3.9, we can use the quadratic score for b and the logarithmic score for S in Proposition 3.10 (ii). This gives the strictly consistent scoring function

$$S(\varrho^{(2)}, \{y_1, \dots, y_m\}) = - \sum_{x_1, x_2 \in \{y_1, \dots, y_m\}}^{\neq} \log(\varrho_0^{(2)}(\|x_1 - x_2\|)) + m^{[2]} \log |\varrho^{(2)}| + c(|\varrho^{(2)}| - m^{[2]})^2,$$

where $c > 0$ is some scaling constant. Simulation experiments in Subsection 5.2 show how S compares different product density forecasts.

3.4 Summary statistics

Summary statistics of point processes are central tools to quantify point interactions such as clustering or inhibition, hence they play a central role in Scenario A or Scenario C1. This subsection constructs strictly consistent scoring functions for the most frequently used statistics, the K - and L -function. Throughout we assume that Φ is not a finite, but a *stationary* point process on \mathbb{R}^d , i.e. any translation of the process by $x \in \mathbb{R}^d$, which we denote via Φ_x , has the same distribution as Φ . This implies that the intensity measure of Φ is a multiple of Lebesgue measure and can be represented via some $\lambda > 0$, see e.g. [Chiu et al. \(2013, Section 4.1\)](#).

A common way to describe a stationary point process is to consider its properties in the neighborhood of $x \in \mathbb{R}^d$, given that x is a point in Φ . Due to stationarity, the location of x is irrelevant and thus it is usually referred to as the “typical point” of Φ . The technical tool to describe the behaviour around this point is the *Palm distribution* of Φ , denoted via \mathbb{P}_0 for probabilities and \mathbb{E}_0 for expectations. It satisfies the defining identity

$$\lambda |W| \mathbb{E}_0 f(\Phi) = \mathbb{E} \left(\sum_{x \in \Phi \cap W} f(\Phi_{-x}) \right)$$

for all measurable functions $f : \mathbb{M}_0 \rightarrow \mathbb{R}$ such that the expectations are finite and it is independent of the observation window $W \in \mathcal{B}(\mathbb{R}^d)$, see e.g. [Illian et al. \(2008, Chapter 4\)](#). Denote the d -dimensional ball of radius $r > 0$ around zero via $B_r = B(0, r)$. The K -function of Φ is defined via

$$K : (0, \infty) \rightarrow [0, \infty), \quad r \mapsto \frac{\mathbb{E}_0 \Phi(B_r \setminus \{0\})}{\lambda},$$

and it quantifies the mean number of points in a ball around the “typical point” of Φ , see e.g. [Chiu et al. \(2013, Chapter 4\)](#) and [Illian et al. \(2008, Chapter 4\)](#). As pointed out by [Heinrich et al. \(2019\)](#) it is unclear whether it is possible to express $K(r)$ as an elicitable property in order to employ Proposition 2.4. We provide a possible solution to this problem by constructing strictly consistent scoring function for reports consisting of both, the K -function and the intensity (see also Example 3.1). Our point process property of interest is thus $\Gamma(P) := (\lambda_P, K_P)$, where the subscript denotes the dependence of the quantities on the distribution $P \in \mathcal{P}$ of the process Φ .

To derive consistent scoring functions let us fix some $r > 0$ and assume for now that λ_P is known and that instead of data we directly observe the Palm distribution of Φ . In this simplified situation, $K_P(r)$ is just an expectation with respect to \mathbb{P}_0 , hence “consistent scoring functions” for it are of the Bregman form

$$b(x, \varphi) = -f(x) - f'(x)(\varphi(B_r \setminus \{0\}) - \lambda_P x), \quad (10)$$

for a convex function $f : (0, \infty) \rightarrow \mathbb{R}$, see Theorem 2.1 and Example 3.1. This is because $\mathbb{E}_{P,0} b(x, \Phi) \geq \mathbb{E}_{P,0} b(K_P(r), \Phi)$ holds for all $x \geq 0$ and $P \in \mathcal{P}$. To arrive at a strictly consistent scoring function for the functional Γ three steps remain: Firstly, we have

to include a consistent scoring function for the first component of Γ , i.e. the intensity. Moreover, we need to integrate (10) with respect to $r > 0$ in order to evaluate the entire K -function. Finally, we have to account for the fact that we can not observe \mathbb{P}_0 , but only points of Φ on some closed and bounded observation window $W \subset \mathbb{R}^d$. Hence, we need to compute the expected score $\mathbb{E}_0 b(x, \Phi)$ via an expectation of Φ on W . Such problems lead to edge corrections, i.e. additional terms to account for the fact that (unobserved) points outside of W affect the estimation near the boundary of W , see e.g. Chiu et al. (2013, Chapter 4.7) for details. Since (10) is linear in φ , edge corrections for the expected score are equivalent to edge corrections for the expectation $\mathbb{E}_0 \Phi(B_r \setminus \{0\})$, which are well-known in the context of K -function estimation. Taken together we obtain the following result.

Proposition 3.12. *Let $b_1, b_2 : [0, \infty) \times [0, \infty) \rightarrow \mathbb{R}$ be (strictly) consistent Bregman functions and $w : (0, \infty) \rightarrow [0, \infty)$ a weight function. Define $\mathcal{C} := \{K_P \mid P \in \mathcal{P}\}$, a set of possible K -functions and let κ satisfy $\mathbb{E}_P \kappa(B_r, \Phi \cap W) = \lambda_P \mathbb{E}_{P,0} \Phi(B_r \setminus \{0\})$ for all $P \in \mathcal{P}$. Then the function $S : ((0, \infty) \times \mathcal{C}) \times \mathbb{M}_0 \rightarrow \mathbb{R}$ defined via*

$$S((\lambda, K), \varphi) = b_1(\lambda, \varphi(W)|W|^{-1}) + \int_0^\infty b_2(\lambda^2 K(r), \kappa(B_r, \varphi))w(r) dr$$

is consistent for the point process property $\Gamma(P) := (\lambda_P, K_P)$ as long as the expectation of the integral is finite. It is strictly consistent if b_1 and b_2 are strictly consistent and w is strictly positive.

Proof. Using Theorem 2.1, the Fubini-Tonelli theorem, and

$$\mathbb{E}_P \kappa(B_r, \Phi) = \lambda_P \mathbb{E}_{P,0} \Phi(B_r \setminus \{0\}) = \lambda_P^2 K_P(r),$$

standard arguments show that the scoring function

$$S'((\lambda, h), \varphi) := b_1(\lambda, \varphi(W)|W|^{-1}) + \int_0^\infty b_2(h(r), \kappa(B_r, \varphi))w(r) dr,$$

where $h : (0, \infty) \rightarrow (0, \infty)$ is an increasing function, is (strictly) consistent for the property $\Gamma'(P) := (\lambda_P, \lambda_P^2 K_P(r))$. An application of the revelation principle (Proposition 2.2) gives (strict) consistency for Γ . \square

Similar to Corollary 3.8, this result blends two scoring components, namely the expected number of points and their distances. Hence, choosing suitable Bregman functions b_1 and b_2 in applications, again leads to issues of balancing the magnitudes of different scoring components.

A similarly intricate question is the choice of κ . Relevant choices result from the construction of estimators for the K -function, which are often based on dividing κ by an estimator for λ^2 , see e.g. Chiu et al. (2013). A common choice is

$$\kappa_{\text{st}}(B_r, \varphi) := \sum_{x_1, x_2 \in \varphi \cap W}^{\neq} \frac{\mathbb{1}_{B_r}(x_2 - x_1)}{|W_{x_1} \cap W_{x_2}|},$$

where $W_z := \{x + z \mid x \in W\}$ is the shifted observation window and r is such that $|W \cap W_z|$ is positive for all $z \in B_r$, see e.g. Illian et al. (2008, Chapter 4.3) and Chiu et al. (2013, Chapter 4.7). An alternative arises via minus-sampling, i.e. by reducing the observation window W in order to reduce edge effects. This yields

$$\kappa_{\text{minus}}(B_r, \varphi) := \frac{1}{|W|} \sum_{x_1, x_2 \in \varphi \cap W, x_2 \in W \ominus r}^{\neq} \mathbb{1}_{B_r}(x_2 - x_1),$$

where $W \ominus r := \{x \mid B(x, r) \subset W\}$ is the reduced observation window. For other choices of κ , most notably for isotropic point processes, see Chiu et al. (2013, Chapter 4.7).

Practitioners usually rely on the L -function, a modification of the K -function, which is defined via $L(r) = \sqrt[d]{K(r)/b_d}$ for $r \geq 0$, where $b_d := |B_1|$. It satisfies $L(r) = r$ for the Poisson point process, and thus normalizes the K -function such that it is independent of the dimension d for a Poisson point process, see e.g. Chiu et al. (2013). A (strictly) consistent scoring function for the L -function follows immediately from Proposition 3.12 and another application of the revelation principle. The explicit formula follows by replacing the first component of b_2 by $\lambda^2 L(r)^d b_d$ in Proposition 3.12. The idea underlying the construction of scoring functions for the K - and L -function presented here can be transferred to other summary statistics for stationary point processes.

3.5 Density and distribution – temporal processes

This subsection turns to consistent scoring functions for temporal point processes and thereby relates to Scenario B, although suitable adaptations to spatio-temporal point processes (Scenario C2) are straightforward. The key feature of temporal (point) processes is that the dimension “time” possesses a natural ordering, which allows for an intuitive conditioning on the past that can be used to obtain explicit temporal point process models.

For temporal processes, the main object of interest is usually the probability of a new point in the process *conditional* on past points. The instantaneous rate of points occurring in the point process Φ is usually described via the *conditional intensity*

$$\lambda^*(t) = \lim_{\Delta t \rightarrow 0} \frac{\mathbb{E}[\Phi((t, t + \Delta t)) \mid \mathcal{H}_t]}{\Delta t}, \quad (11)$$

where $(\mathcal{H}_t)_{t \in \mathbb{R}}$ is the filtration generated by the history of Φ , see e.g. Reinhart (2018). Although $\lambda^*(t)$ is random, it is known conditional on Φ , hence a measurable mapping linking it to Φ allows for modeling as well as evaluation via consistent scoring functions. This mapping is usually based on the concept of *hazard functions* which also reflects a fruitful perspective in applications (Harte, 2015; Reinhart, 2018). We turn to an illustrative example and refer to Daley and Vere-Jones (2003, Chapter 7) for further details.

Example 3.13 (Hawkes process). This basic *self-exciting* point process model was proposed by Hawkes (1971) and is defined via the conditional intensity

$$\lambda^*(t) = \nu + \sum_{t_i < t} g(t - t_i),$$

where $\nu \geq 0$ is the *background rate*, $g : (0, \infty) \rightarrow [0, \infty)$ is the *triggering function*, and $(t_i)_{i \in \mathbb{N}}$ comprises the points of the point process Φ . For a review of its applications see for instance [Reinhart \(2018\)](#).

Let Φ be a point process on \mathbb{R}_+ and consider an observation window $\mathcal{X} := [0, T]$ for some $T > 0$. Given a realization $0 < t_1 < \dots < t_n$ of Φ the realized values of the conditional intensity can be computed for all $t \in \mathcal{X}$. More precisely, for a $t \in \mathcal{X}$ with $t_1 < \dots < t_i \leq t < t_{i+1}$ we denote the realized value of λ^* at t via $\lambda^*(t \mid t_1, \dots, t_i)$. Whenever there is no need to emphasize the dependence on t_1, \dots, t_i we use the simpler notation $\lambda^*(t)$. To ensure uniqueness, we follow [Daley and Vere-Jones \(2003\)](#) and assume that a left-continuous version of λ^* exists and is used.

Since the collection of all mappings $t \mapsto \lambda^*(t \mid t_1, \dots, t_i)$ for all $i = 0, \dots, n$ and all possible realizations t_1, \dots, t_n uniquely determines the distribution of Φ ([Daley and Vere-Jones, 2003](#)), comparing forecasts for the conditional intensity is equivalent to a comparison of forecasts for the distribution. The connection is the representation of the likelihood of t_1, \dots, t_n occurring in $[0, T]$ via

$$j_n(t_1, \dots, t_n) = \left(\prod_{i=1}^n \lambda^*(t_i) \right) \exp \left(- \int_0^T \lambda^*(u) du \right), \quad (12)$$

where the product is interpreted as one if no points occur. Consequently, (strictly) consistent scoring functions for the conditional intensity can be obtained via similar arguments as in Subsection 3.2, as illustrated by the following example.

Example 3.14. The logarithmic score is the most intuitive choice of strictly consistent scoring function for point process densities. Plugging (12) into (7) we see that the scoring function S given by

$$S(\lambda^*, \{t_1, \dots, t_n\}) = - \sum_{i=1}^n \log(\lambda^*(t_i)) + \int_0^T \lambda^*(u) du,$$

is strictly consistent for the conditional intensity. This recovers the log-likelihood of a temporal point process, see for instance [Daley and Vere-Jones \(2003\)](#) and [Reinhart \(2018\)](#). If Φ is a Poisson point process on \mathbb{R}_+ with intensity λ , its conditional intensity agrees with λ and S coincides with (8). Simulation experiments in Subsection 5.3 illustrate how S compares different forecasts of conditional intensities of Hawkes processes.

Instead of using the likelihood (12) for scoring, an alternative is to proceed stepwise and compute the distribution of the next point conditional on all previous points. After doing this for all points the resulting distributions are then evaluated via consistent scoring functions. The conditional probability density and distribution function of the point t_i , given t_1, \dots, t_{i-1} are

$$f_i(t \mid t_1, \dots, t_{i-1}) = \lambda^*(t \mid t_1, \dots, t_{i-1}) \exp \left(- \int_{t_{i-1}}^t \lambda^*(u \mid t_1, \dots, t_{i-1}) du \right) \quad \text{and}$$

$$F_i(t \mid t_1, \dots, t_{i-1}) = 1 - \exp \left(- \int_{t_{i-1}}^t \lambda^*(u \mid t_1, \dots, t_{i-1}) \, du \right),$$

where $t \in (t_{i-1}, \infty)$. For $i = 0$ the functions are unconditional and we use the convention $t_0 = 0$. The collection of these conditional distributions gives an equivalent characterization of the point process distribution P_Φ , see [Daley and Vere-Jones \(2003, Chapter 7.2\)](#) for details. Let \mathcal{D} be the set of left-continuous positive mappings on $[0, T)$. Adding the scores for all intervals gives the following result.

Proposition 3.15. *Let $S_i : \mathcal{F} \times [0, \infty) \rightarrow \mathbb{R}$ for $i \in \mathbb{N}$ be (strictly) consistent scoring functions for densities and $S' : [0, 1] \times \{0, 1\} \rightarrow \mathbb{R}$ a (strictly) consistent scoring function for Bernoulli distributions. Then the scoring function $S : \mathcal{D} \times \mathbb{M}_0 \rightarrow \mathbb{R}$ defined via*

$$S(\lambda^*, \{t_1, \dots, t_n\}) = \sum_{i=1}^n S_i(f_i(\cdot \mid t_1, \dots, t_{i-1}), t_i) + S'(1 - F_{n+1}(T \mid t_1, \dots, t_n), 1)$$

for $n \in \mathbb{N}$ and $S(\lambda^*, \emptyset) = S'(1 - F_1(T), 1)$ is consistent for the conditional intensity restricted to $[0, T]$. It is strictly consistent, if all $(S_i)_{i \in \mathbb{N}}$ and S' are strictly consistent.

Proof. By the tower property of conditional expectations, the expectation of S_i is the mean of the conditional expectation given t_1, \dots, t_{i-1} for every $i = 2, \dots, n$. Consequently, the reported conditional distributions are compared to the true conditional distributions in expectation. An analogous argument for S' shows (strict) consistency. \square

The scoring function S' in Proposition 3.15 evaluates the forecast probability of an empty interval occurring after t_n . Since it is possible to choose a different scoring function S_i for every point t_i , this result leads to a greater variety of scoring functions for temporal point processes than the likelihood approach of Subsection 3.2. Choosing the logarithmic score for all $(S_i)_{i \in \mathbb{N}}$ and S' recovers the scoring function of Example 3.14 and thereby connects both approaches.

Another benefit of Proposition 3.15 becomes apparent when considering marked point processes. In this setting points t_i and corresponding marks κ_i are observed and the conditional intensity admits the decomposition $\lambda^*(t, \kappa) = \lambda_g^*(t) \psi^*(\kappa \mid t)$, where λ_g^* is the conditional intensity of the ground process and $\psi^*(\cdot \mid t)$ is the conditional density of the marks. Just like λ^* , $\psi^*(\cdot \mid t)$ is a random variable depending on the realized points and marks prior to t , see [Daley and Vere-Jones \(2003, Chapter 7.3\)](#) for details. If both functions are reported, a consistent scoring function for λ^* emerges by using S as given in Proposition 3.15 for λ_g^* and adding scores for the marks. More precisely, such a scoring function is of the form

$$\begin{aligned} \tilde{S}((\lambda_g^*, \psi^*), \{t_1, \dots, t_n\}, \{\kappa_1, \dots, \kappa_n\}) &= S(\lambda_g^*, \{t_1, \dots, t_n\}) \\ &\quad + \sum_{i=1}^n S_i^m(\psi^*(\cdot \mid t_1, \dots, t_i, \kappa_1, \dots, \kappa_{i-1}), \kappa_i), \end{aligned}$$

where $(S_i^m)_{i \in \mathbb{N}}$ are (strictly) consistent scoring functions for the mark densities. These additional scores evaluate each density $\psi^*(\cdot | t)$ given a point at t . A decomposed scoring function such as \tilde{S} might be beneficial in applications where different scoring functions for the points and marks are reasonable. For instance, only some distributional properties of ψ^* , e.g. the tails, might be of interest and the $(S_i^m)_{i \in \mathbb{N}}$ can be tailored to emphasize this.

4 Review of extant methods for model comparison

This section discusses existing techniques for the evaluation of point process models and how they relate to consistent scoring functions. We distinguish two model evaluation approaches common in statistical seismology, and discuss how they can be interpreted as scoring function-based comparison methods. Due to this emphasis, other concepts which do not primarily aim at comparative evaluation, e.g. diagnostic tools, are omitted.

A standard approach to model comparison consists of using the log-likelihood of a model, i.e. its log-density evaluated at the observations. Most prominently, information criteria such as the AIC or BIC build on this idea to assess the relative quality of competing models, and they can also be used for point process models, as long as likelihoods are available, see e.g. [Chen et al. \(2018\)](#). Information criteria connect naturally to consistent scoring functions through their goodness-of-fit component which usually consists of a log-likelihood and can thus be interpreted as evaluating the logarithmic score (5) for the given model. The penalty component, which is computed from the number of fitted parameters, highlights the difference to consistent scoring functions. It is a necessary correction for information criteria, as their comparison is in-sample, i.e. it relies on the same data which is used for model fitting. In contrast, comparative forecast evaluation via scoring functions is ideally performed using new data which was not previously used to fit models or issue forecasts. We refer to [Gneiting and Raftery \(2007, Section 7\)](#) for further aspects of this connection.

In the Bayesian setting a standard approach to model comparison is the use of *Bayes factors*, which indicate whether there is sufficient evidence for one model to be more likely than a competitor. Like information criteria they are closely connected to the logarithmic score (5), as discussed in [Gneiting and Raftery \(2007, Section 7\)](#). [Marzocchi et al. \(2012\)](#) employ Bayes factors to compare point process models in the setting of earthquake likelihood model testing (Subsection 4.2).

A further variant of the likelihood principle for point processes can be obtained from a combination with residual methods. In general, point process residuals form an empirical process arising from fitting a conditional intensity (see Subsection 3.5) to data. They can be used to assess goodness-of-fit and especially indicate in which regions a model fits well or poorly, see e.g. [Bray and Schoenberg \(2013\)](#) for a review. [Clements et al. \(2011\)](#) propose the use of deviance residuals to graphically compare two competing models for the conditional intensity of a spatio-temporal process. The method plots the log-likelihood ratio of two models for every set of a partition of the spatial domain and can thus be interpreted as a visualization of local differences in logarithmic score.

4.1 Information gain

Closely connected to log-likelihood methods is the information gain approach, introduced by Vere-Jones (1998) as a tool to compare temporal point processes (Scenario B). The main idea is to assess a model based on the event probabilities that it induces for a collection of intervals. Although the term ‘information gain’ is sometimes used in the context of spatial point processes, too (Rhoades et al., 2011; Strader et al., 2017), we focus on the temporal case and consider a spatial analogon in the next subsection.

The basis for the information gain is a partition of the interval $[0, T]$ into n subintervals with length δ_i for $i = 1, \dots, n$. A distributional model for a point process Φ , i.e. a distribution $P \in \mathcal{P}$ can then be used to generate (conditional) probabilities for the event that at least one point occurs in interval i . Assume two collections of such probabilities $(p_i)_{i=1, \dots, n}$ and $(q_i)_{i=1, \dots, n}$ are given, where the former is computed from the model under consideration and the latter corresponds to a reference model, usually a homogeneous Poisson process. The time-normalized log-likelihood ratio between $(p_i)_{i=1, \dots, n}$ and $(q_i)_{i=1, \dots, n}$ is

$$\bar{\rho}_T = \frac{1}{T} \sum_{i=1}^n \left[X_i \log \left(\frac{p_i}{q_i} \right) + (1 - X_i) \log \left(\frac{1 - p_i}{1 - q_i} \right) \right], \quad (13)$$

where the X_i are binary random variables indicating whether or not interval i contains a point of Φ , see Daley and Vere-Jones (2003, Chapter 7.6). This term is called *mean information gain per unit time* by Vere-Jones (1998) and positive values are assumed to indicate improved forecast performance of the model compared to the reference model. How this connects to scoring functions is presented in Subsection 4.3.

When using the information gain method, the choice of suitable subintervals is crucial, as this will influence the performance measured by $\bar{\rho}_T$. The impact of different choices is difficult to assess, however, Vere-Jones (1998) and Daley and Vere-Jones (2003, Chapter 7.6) show that the maximal gain is independent of the choice of intervals. More precisely, let Φ be a stationary temporal point process with conditional intensity function λ^* and X_i Bernoulli variables with parameters p_i for $i = 1, \dots, n$. If q_i is computed from a homogeneous Poisson point process with rate $\bar{\lambda}$ given by the mean intensity $\bar{\lambda} := \mathbb{E}[\lambda^*(0)]$, i.e. via $q_i = 1 - \exp(-\bar{\lambda}\delta_i)$, then $\mathbb{E}\bar{\rho}_T$ is bounded by

$$\mathcal{I} := \mathbb{E}[\lambda^*(0) \log(\lambda^*(0))] - \bar{\lambda} \log(\bar{\lambda}),$$

the *entropy gain per unit time* of the process. Moreover, $\mathbb{E}\bar{\rho}_T \rightarrow \mathcal{I}$ for a refining sequence of partitions of $[0, T]$. Due to this result, \mathcal{I} can be interpreted as the ‘predictability’ of the process Φ by measuring the potential for concentration in contrast to the homogeneous Poisson process with rate equal to the mean intensity, see e.g. Vere-Jones (1998) and Daley and Vere-Jones (2004). This quantification of predictability via \mathcal{I} may also be used for a goodness-of-fit criterion, where \mathcal{I} is estimated from the data via the information gain (13) and compared to the true value for a given model, see Daley and Vere-Jones (2004) and Harte and Vere-Jones (2005) for details.

4.2 Earthquake likelihood model testing

When considering spatial point processes, as in our Scenario A, explicitly computable likelihoods are often not available. A major exception are Poisson point processes, which motivates a model evaluation approach by [Kagan and Jackson \(1995\)](#) and [Schorlemmer et al. \(2007\)](#), to which we refer as ‘earthquake likelihood model testing’. Together with further conceptual and computational improvements due to [Zechar et al. \(2010\)](#) and [Rhoades et al. \(2011\)](#) this method is used in the RELM initiative, where a collection of earthquake forecasts underwent several prospective testing procedures, see [Schorlemmer and Gerstenberger \(2007\)](#) for details.

Earthquake likelihood model testing represents each earthquake by a point in $\mathbf{S} \times \mathbf{M}$, where $\mathbf{S} \subset \mathbb{R}^k$ is some region in space and $\mathbf{M} \subset \mathbb{R}^d$ is a set of marks, representing earthquake features such as magnitude. The set $\mathbf{S} \times \mathbf{M}$ is partitioned into bins B_1, \dots, B_N for some $N \in \mathbb{N}$ and the values $x_1, \dots, x_N \in \mathbb{N}_0$ count the numbers of earthquakes falling in each bin. A forecast or ‘model’ is determined by values $\lambda_1, \dots, \lambda_N \in (0, \infty)$ and its ‘log-likelihood’ ([Schorlemmer et al., 2007](#)) is defined as a sum of Poisson likelihoods

$$\ell(\lambda_1, \dots, \lambda_N, x_1, \dots, x_N) = \sum_{i=1}^N (x_i \log \lambda_i - \log(x_i!) - \lambda_i). \quad (14)$$

This terminology is motivated by the fact that, if Φ is a Poisson point process with intensity measure Λ such that $\Lambda(B_i) = \lambda_i$ for $i = 1, \dots, N$, then (14) is the log-likelihood of the realization x_1, \dots, x_N . Based on this idea, [Kagan and Jackson \(1995\)](#) and [Schorlemmer et al. \(2007\)](#) propose different tests to evaluate forecasts.

To assess the absolute performance of a forecast, they introduce the *L-test*, which compares the realized value $z := \ell(\lambda_1, \dots, \lambda_N, x_1, \dots, x_N)$ to the distribution of the random variable $Z := \ell(\lambda_1, \dots, \lambda_N, X_1, \dots, X_N)$, where X_1, \dots, X_N are independent Poisson random variables with parameters $\lambda_1, \dots, \lambda_N$. The model is rejected if the realization z lies in the tail of the distribution of Z . To determine the latter, we can either rely on simulations or approximate the CDF of Z , as proposed in [Rhoades et al. \(2011\)](#).

The *R-test*, or ratio test, compares two forecasts A and B specified by their bin intensities λ_i^A and λ_i^B for $i = 1, \dots, N$, and aims to check whether model A is at least as good as model B . Naturally, the analogous formulation with reversed roles is possible, as well. The R-test considers the ‘log-likelihood ratio’ based on (14), i.e.

$$R(A, B, x_1, \dots, x_N) = \ell(\lambda_1^A, \dots, \lambda_N^A, x_1, \dots, x_N) - \ell(\lambda_1^B, \dots, \lambda_N^B, x_1, \dots, x_N), \quad (15)$$

and then proceeds analogously to the L-test, i.e. it compares the realized value $z := R(A, B, x_1, \dots, x_N)$ to the distribution of the random variable $Z := R(A, B, X_1, \dots, X_N)$, where X_1, \dots, X_N are independent Poisson random variables with parameters λ_i^A for $i = 1, \dots, N$. If z lies in the lower tail of the distribution of Z , then model A is deemed worse than model B .

As the distributional assumptions on X_1, \dots, X_N demonstrate, there is an asymmetry inherent in the R-test: If model A is tested against model B , then the X_i are assumed to

have parameters λ_i^A and if B is tested against A , then λ_i^B are assumed for X_i . As noted by Rhoades et al. (2011) this implies that the R-test is not really a comparative test, but rather a goodness-of-fit test such as the L-test. This explains seemingly contradictory results observed in practice, where R-tests deem A worse than B and vice versa, see Rhoades et al. (2011) and Bray and Schoenberg (2013) for details and references.

Motivated by this asymmetry, Rhoades et al. (2011) propose two modifications of the R-test which avoid such contradictory results. Instead of assuming a distribution for (15), they find a different representation of R and assume a normal distribution for this test statistic. Large positive realizations of R then support model A , while large negative values support model B . If too few data are available they propose to test whether R has zero median by employing the Wilcoxon signed-rank test. Both testing ideas can be interpreted as variants of Diebold-Mariano (DM) tests (see Diebold and Mariano (1995) and Subsection 2.2) and the connection to scoring functions is detailed in Subsection 4.3. Note that Rhoades et al. (2011) use the term ‘information gain’ to refer to their test statistic, see Subsection 4.1.

As pointed out by Harte (2015), earthquake likelihood model testing suffers from several drawbacks. Firstly, relying on binning leads to a loss of information, since the behavior of models inside bins will not affect the evaluation. Moreover, assuming independence among bins as well as a Poisson distribution leads to a likelihood misspecification when assessing general point process models. This prohibits the testing of model characteristics other than bin expectations, since by reporting $(\lambda_i)_{i=1,\dots,n}$, every forecast is converted to a Poisson point process. The Collaboratory for the Study of Earthquake Predictability (CSEP), which succeeds RELM, will address these problems by considering more complex forecasts, which include distributional features or correlations, see Schorlemmer et al. (2018) for details. However, as mentioned by Bray and Schoenberg (2013), it is unclear how big the impact of the Poisson assumption is on the testing results. By viewing the testing methods from the perspective of consistent scoring functions, the next subsection gives new insights into this question.

4.3 Connections to scoring theory

The ideas of information gain and earthquake likelihood model testing can be interpreted as special choices of consistent scoring functions which compare a collection of forecasts and realizations for each set in a partition \mathcal{T} of the domain \mathcal{X} .

Information gain We start with Scenario B and consider a temporal point process on an interval $[0, T]$ and a partition of $(0, T]$ into k_n subintervals via $\mathcal{T}_n := \{(a_1, b_1], \dots, (a_{k_n}, b_{k_n}]\}$, $n \in \mathbb{N}$. Motivated by the information gain approach in Subsection 4.1 we define the *interval scoring function* $S_{\text{int}}^{\mathcal{T}_n} : [0, 1]^{k_n} \times \mathbb{M}_0 \rightarrow \mathbb{R}$ via

$$S_{\text{int}}^{\mathcal{T}_n}(p_1, \dots, p_{k_n}, \varphi) = \sum_{i=1}^{k_n} [-\mathbb{1}(\varphi((a_i, b_i]) > 0) \log(p_i) - \mathbb{1}(\varphi((a_i, b_i]) = 0) \log(1 - p_i)] \quad (16)$$

for each partition \mathcal{T}_n , $n \in \mathbb{N}$. The summands of (13) equal $S(q_i, X_i) - S(p_i, X_i)$, where $X_i := \mathbb{1}(\Phi((a_i, b_i]) > 0)$ and $S : [0, 1] \times \{0, 1\} \rightarrow \mathbb{R}$ defined via

$$S(p, y) = -y \log(p) - (1 - y) \log(1 - p) \quad (17)$$

is the binary logarithmic score. Since S is a strictly consistent scoring function for the probability $\mathbb{P}(Y = 1)$ (Gneiting and Raftery, 2007), we obtain that $S_{\text{int}}^{\mathcal{T}_n}$ is strictly consistent for the collection of probabilities $\mathbb{P}(\Phi((a_i, b_i]) > 0)$ with $(a_i, b_i] \in \mathcal{T}_n$. Hence, we can loosely speak of *negative* information gains as being strictly consistent for the collection of probabilities that interval i contains at least one point of Φ . This holds for unconditional as well as conditional probabilities alike. For conditional probabilities forecasters need to report instructions on how to calculate the probabilities from past observations. Simulation experiments in Subsection 5.3 illustrate how this approach compares different conditional intensity forecasts.

If conditional probabilities can be computed from a conditional intensity model λ^* , then $S_{\text{int}}^{\mathcal{T}_n}$ connects naturally to the scoring functions derived in Subsection 3.5. To make this precise, we follow Daley and Vere-Jones (2003, Definition A1.6.I) and call a sequence of partitions $(\mathcal{T}_n)_{n \in \mathbb{N}}$ *dissecting* if it is nesting and asymptotically separates every pair of points. Then we obtain the following approximation result. Subsection 5.3 studies the quality of this approximation via simulations.

Proposition 4.1. *Let λ^* be a conditional intensity and $(\mathcal{T}_n)_{n \in \mathbb{N}}$ a dissecting system of partitions of $(0, T]$ consisting of intervals. Let $P_0 \in \mathcal{P}$ be the distribution of the unit rate Poisson point process on $[0, T]$ and define conditional probability reports*

$$p_i^{(n)} = 1 - \exp \left(- \int_{a_i^{(n)}}^{b_i^{(n)}} \lambda^*(t \mid t_j < a_i^{(n)}) dt \right)$$

for all $i = 1, \dots, k_n$, $(a_i^{(n)}, b_i^{(n)}] \in \mathcal{T}_n$, and $n \in \mathbb{N}$. Then

$$S_{\text{int}}^{\mathcal{T}_n}(p_1^{(n)}, \dots, p_N^{(n)}, \varphi) + \sum_{i=1}^{k_n} \mathbb{1}(\varphi((a_i^{(n)}, b_i^{(n)}]) > 0) \log(b_i^{(n)} - a_i^{(n)}) \longrightarrow S(\lambda^*, \varphi),$$

for P_0 -a.e. $\varphi \in \mathbb{M}_0([0, T])$ as $n \rightarrow \infty$, where S is the scoring function from Example 3.14.

Proof. Denote a point process realization via $\varphi = \{t_1, \dots, t_m\}$ for $m \in \mathbb{N}_0$ and let n be large enough so that each interval contains at most one point. Let $I_0^{(n)} \subset \{1, \dots, k_n\}$ denote the indices of intervals which do not contain a point and $I_1^{(n)}$ the indices of intervals which contain a point. The score $S_{\text{int}}^{\mathcal{T}_n}(p_1^{(n)}, \dots, p_N^{(n)}, \varphi)$ can now be divided into two sums with respect to the indices $I_0^{(n)}$ and $I_1^{(n)}$. For the first sum we obtain

$$\sum_{i \in I_0^{(n)}} -\mathbb{1}(\varphi((a_i^{(n)}, b_i^{(n)}]) = 0) \log(1 - p_i^{(n)}) = \sum_{i \in I_0^{(n)}} \int_{a_i^{(n)}}^{b_i^{(n)}} \lambda^*(t \mid t_j < a_i^{(n)}) dt.$$

For the second sum we add the correction term and use the fact that $|\log(1 - \exp(-x)) - \log(x)| \rightarrow 0$ for $x \rightarrow 0$. This yields

$$\begin{aligned} & \sum_{i \in I_1^{(n)}} -\mathbb{1}(\varphi((a_i^{(n)}, b_i^{(n)}]) > 0) \log(p_i^{(n)}) + \sum_{i=1}^{k_n} \mathbb{1}(\varphi((a_i^{(n)}, b_i^{(n)}]) > 0) \log(b_i^{(n)} - a_i^{(n)}) \\ &= \sum_{i \in I_1^{(n)}} -\log \left((b_i^{(n)} - a_i^{(n)})^{-1} \int_{a_i^{(n)}}^{b_i^{(n)}} \lambda^*(t \mid t_j < a_i^{(n)}) dt \right) + o(1) \\ &\rightarrow -\sum_{j=1}^m \log(\lambda^*(t_j \mid t_1, \dots, t_{j-1})) \end{aligned}$$

for $n \rightarrow \infty$ and P_0 -a.e. $\varphi \in \mathbb{M}_0([0, T])$. The convergence follows from suitable approximation results for λ^* , see e.g. [Daley and Vere-Jones \(2003, Lemma A1.6.III\)](#). Combined with the first equation this gives the result. \square

Earthquake likelihood model testing In earthquake likelihood model testing (Subsection 4.2) forecasts consist of positive values $\lambda_1, \dots, \lambda_n$, and the corresponding Poisson distributions are compared via the logarithmic score. To formalize this, consider a bounded spatial domain \mathcal{X} which is partitioned into k_n bins $\mathcal{T}_n = \{B_1, \dots, B_{k_n}\}$. Based on (14) and (15) we define the *bin scoring function* $S_{\text{bin}}^{\mathcal{T}_n} : (0, \infty)^{k_n} \times \mathbb{M}_0 \rightarrow \mathbb{R}$ via

$$S_{\text{bin}}^{\mathcal{T}_n}(\lambda_1, \dots, \lambda_{k_n}, \varphi) = \sum_{i=1}^{k_n} -\varphi(B_i) \log(\lambda_i) + \lambda_i \quad (18)$$

for each partition \mathcal{T}_n , $n \in \mathbb{N}$. The following result establishes that $S_{\text{bin}}^{\mathcal{T}_n}$ is strictly consistent for the collection of bin expectations $\mathbb{E}\Phi(B_i)$, $B_i \in \mathcal{T}_n$, see also Example 3.1.

Proposition 4.2. *If \mathcal{N} is a set of probability measures on \mathbb{N}_0 with finite first moments, then the scoring function $S : (0, \infty) \times \mathbb{N}_0 \rightarrow \mathbb{R}$ defined via*

$$S(\lambda, y) = -y \log(\lambda) + \lambda \quad (19)$$

is strictly consistent for the expectation.

Proof. Since S is the Bregman function corresponding to the strictly convex function $f(\lambda) = \lambda(\log(\lambda) - 1)$, the assertion follows from Theorem 2.1. \square

The scoring function (19) can be interpreted as a discrete analogon to the David-Sebastiani-score ([Dawid and Sebastiani, 1999](#)), but with the normal distribution replaced by the Poisson distribution. The term $\log(y!)$ which appears in (14) can be omitted, since it does not depend on the report λ .

As noted by [Harte \(2015\)](#) the implications of using Poisson likelihoods for earthquake likelihood model testing are not completely clear. Via Proposition 4.2 we now see that

the Poisson assumption leads to a sound comparison of bin expectations, since the true expectations obtain minimal expected score. This conclusion holds even if the data do not follow a Poisson point process. Hence, the Poisson assumption does not imply that the corresponding tests are only valid for Poisson point process data. It rather means that the tests are sensitive to the bin expectations only, since they rely on strictly consistent scoring functions for the expectation. As a consequence, the symmetric modifications of the R-test due to Rhoades et al. (2011), which assume a normal distribution for the log-likelihood ratio (15), can be seen as DM tests in the spirit of Subsection 2.2, based on the scoring function $S_{\text{bin}}^{\mathcal{T}_n}$.

Just as the Poisson distribution gives rise to the scoring function (19) for the expectations, the Poisson point process can be used to obtain a scoring function for the intensity. The reason is that every intensity report induces a Poisson point process with this intensity and these processes can then be compared via the logarithmic score (7), which attains the value (8) for Poisson densities. Using the notation from Subsection 3.3 we obtain strict consistency, analogous to Proposition 4.2.

Proposition 4.3. *Let all elements of \mathcal{M}_f admit densities with respect to Lebesgue measure. Then the scoring function $S : \mathcal{M}_f \times \mathbb{M}_0 \rightarrow \mathbb{R}$ defined via*

$$S(\Lambda, \{y_1, \dots, y_n\}) = - \sum_{i=1}^n \log \lambda(y_i) + \int_{\mathcal{X}} \lambda(y) \, dy \quad (20)$$

for $n \in \mathbb{N}$ and $S(\Lambda, \emptyset) = \int \lambda(y) \, dy$ is a strictly consistent scoring function for the intensity.

Proof. The scoring function (20) corresponds to an S from Corollary 3.8 when choosing the logarithmic score for S' , the Bregman function b as in the proof of Proposition 4.2, and $c = 1$. Since S' and b are both strictly consistent, S is strictly consistent for the intensity. \square

The scoring function (20) can be interpreted as a point process analogon to the Dawid-Sebastiani-score (Dawid and Sebastiani, 1999). While the Dawid-Sebastiani-score relies on the first and second moments of the predictive distribution, this score depends on the intensity only.

Proposition 4.3 shows that a straightforward generalization of earthquake likelihood model testing, which compares general processes via their Poisson point process counterparts, leads to a consistent comparison of intensities. In particular, we can conclude that binning is not necessary for this approach. Intensities can be modelled without relying on bins and they can be compared via scoring functions for intensities (see Subsection 3.3) with Proposition 4.3 giving one possible choice.

However, in some situations binning might be desirable, e.g. when no explicit expression for λ is available. The next result shows that under weak conditions $S_{\text{bin}}^{\mathcal{T}_n}$ can be used as an approximation to the scoring function (20) in this situation.

Proposition 4.4. *Let $\lambda : \mathcal{X} \rightarrow (0, \infty)$ be an intensity and $(\mathcal{T}_n)_{n \in \mathbb{N}}$ a dissecting system of partitions of \mathcal{X} , consisting of rectangles. Let $P_0 \in \mathcal{P}$ be the distribution of the unit rate Poisson point process on \mathcal{X} and define reports*

$$\lambda_i^{(n)} = \int_{B_i^{(n)}} \lambda(y) \, dy,$$

for all $i = 1, \dots, k_n$, $B_i^{(n)} \in \mathcal{T}_n$, and $n \in \mathbb{N}$. Then

$$S_{\text{bin}}^{\mathcal{T}_n}(\lambda_1^{(n)}, \dots, \lambda_{k_n}^{(n)}, \varphi) + \sum_{i=1}^{k_n} \mathbb{1}(\varphi(B_i^{(n)}) > 0) \log(|B_i^{(n)}|) \longrightarrow S(\Lambda, \varphi),$$

for P_0 -a.e. $\varphi \in \mathbb{M}_0$ as $n \rightarrow \infty$, where S is the scoring function (20).

Proof. Let $\varphi = \{y_1, \dots, y_m\}$ with $m \in \mathbb{N}_0$ be a point process realization. For a large enough $n \in \mathbb{N}$ every bin $B_i^{(n)}$ contains at most one point of φ so let $i_n(j)$ denote the index of the bin such that $y_j \in B_{i_n(j)}^{(n)}$ for all $j = 1, \dots, m$. This yields

$$\begin{aligned} S_{\text{bin}}^{\mathcal{T}_n}(\lambda_1^{(n)}, \dots, \lambda_{k_n}^{(n)}, \varphi) &+ \sum_{i=1}^{k_n} \mathbb{1}(\varphi(B_i^{(n)}) > 0) \log(|B_i^{(n)}|) \\ &= - \sum_{i=1}^{k_n} \left[\varphi(B_i^{(n)}) \log \left(\int_{B_i^{(n)}} \lambda(y) \, dy \right) - \mathbb{1}(\varphi(B_i^{(n)}) > 0) \log(|B_i^{(n)}|) - \int_{B_i^{(n)}} \lambda(y) \, dy \right] \\ &= - \sum_{j=1}^m \log \left(|B_{i_n(j)}^{(n)}|^{-1} \int_{B_{i_n(j)}^{(n)}} \lambda(y) \, dy \right) + \int_{\mathcal{X}} \lambda(y) \, dy \\ &\longrightarrow - \sum_{j=1}^m \log(\lambda(y_j)) + \int_{\mathcal{X}} \lambda(y) \, dy \end{aligned}$$

for $n \rightarrow \infty$ and P_0 -a.e. $\varphi \in \mathbb{M}_0$. The last line follows from suitable approximation results for the Radon-Nikodým derivative λ , see e.g. Daley and Vere-Jones (2003, Lemma A1.6.III). \square

This result can be proved for more general partitions, as long as the family of sets $(\mathcal{T}_n)_{n \in \mathbb{N}}$ generates the Borel σ -algebra on \mathcal{X} . However, in most cases of interest partitions which arise from binning each coordinate into intervals will probably suffice. Subsection 5.1 studies the speed of convergence of this binning approach via simulation experiments.

5 Simulation examples

This section investigates finite sample properties of scoring function-based model evaluation, by illustrating the behavior of average score differences and Diebold-Mariano

Table 2: Fraction of times the ‘row forecast’ was preferred over the ‘column forecast’ by a standard DM test with level $\alpha = 0.05$, where Φ is a Poisson point process (left) or a Gaussian determinantal point process (right)

	f_0	f_1	f_2	f_3	f_4	f_5		f_0	f_1	f_2	f_3	f_4	f_5
f_0		0.46	0.84	0.66	1.00	1.00	f_0		0.57	0.89	0.76	1.00	1.00
f_1	0.00		0.40	0.64	0.99	1.00	f_1	0.00		0.45	0.73	0.99	1.00
f_2	0.00	0.00		0.29	0.96	1.00	f_2	0.00	0.01		0.38	0.97	1.00
f_3	0.00	0.00	0.00		0.49	1.00	f_3	0.00	0.00	0.00		0.55	1.00
f_4	0.00	0.00	0.00	0.00		1.00	f_4	0.00	0.00	0.00	0.00		1.00
f_5	0.00	0.00	0.00	0.00	0.00		f_5	0.00	0.00	0.00	0.00	0.00	

(DM) tests for different models and scenarios. We begin with spatial point processes and consider the intensity and the product density (Subsection 3.3). We compare different forecasts for both characteristics based on $N \in \mathbb{N}$ realizations of the point process, where N could reflect a number of different sampling areas (Scenario A) or different time windows (Scenario C1), e.g. $N = 52$ for one year of weekly data. We then turn to temporal processes (Scenario B) and compare forecasts of the triggering properties of linear Hawkes processes (Subsection 3.5) based on one realization of the process in an interval $[0, T]$.

All simulations are performed with the free software R (R Core Team, 2020). We use the `spatstat` package (Baddeley and Turner, 2005; Baddeley et al., 2015) for the spatial point processes and Ogata’s thinning method (Ogata, 1981) for the temporal point processes.

5.1 Intensity

This subsection compares different intensity reports based on average scores for a point process Φ on the window $[0, 1]^2$, which corresponds to Scenario A. We draw $N = 20$ i.i.d. samples φ_i from Φ and compare the average score $\bar{s}_j := \frac{1}{N} \sum_{i=1}^N S(f_j, \varphi_i)$ for different forecast intensities f_j . We consider four different data-generating processes for Φ all of which have (approximate) intensity $\lambda(x, y) = 30\sqrt{x^2 + y^2}$. The simulations are repeated $M = 500$ times to assess the variation in average scores.

Six different intensity forecasts are compared below, namely the perfect forecast $f_0 = \lambda$ and

$$\begin{aligned}
 f_1(x, y) &= 40\sqrt{(x - 0.2)^2 + (y - 0.1)^2} \\
 f_2(x, y) &= 11.78(x + 3y) \\
 f_3(x, y) &= 45\sqrt{(x - 0.2)^2 + (y - 0.1)^2} \\
 f_4(x, y) &= 9.5 \left(\frac{1}{\sqrt{1.2 - x}} + 2(1 - y) \right) \\
 f_5(x, y) &= 46 \exp(-2(x^2 + (y - 1/2)^2))
 \end{aligned}$$

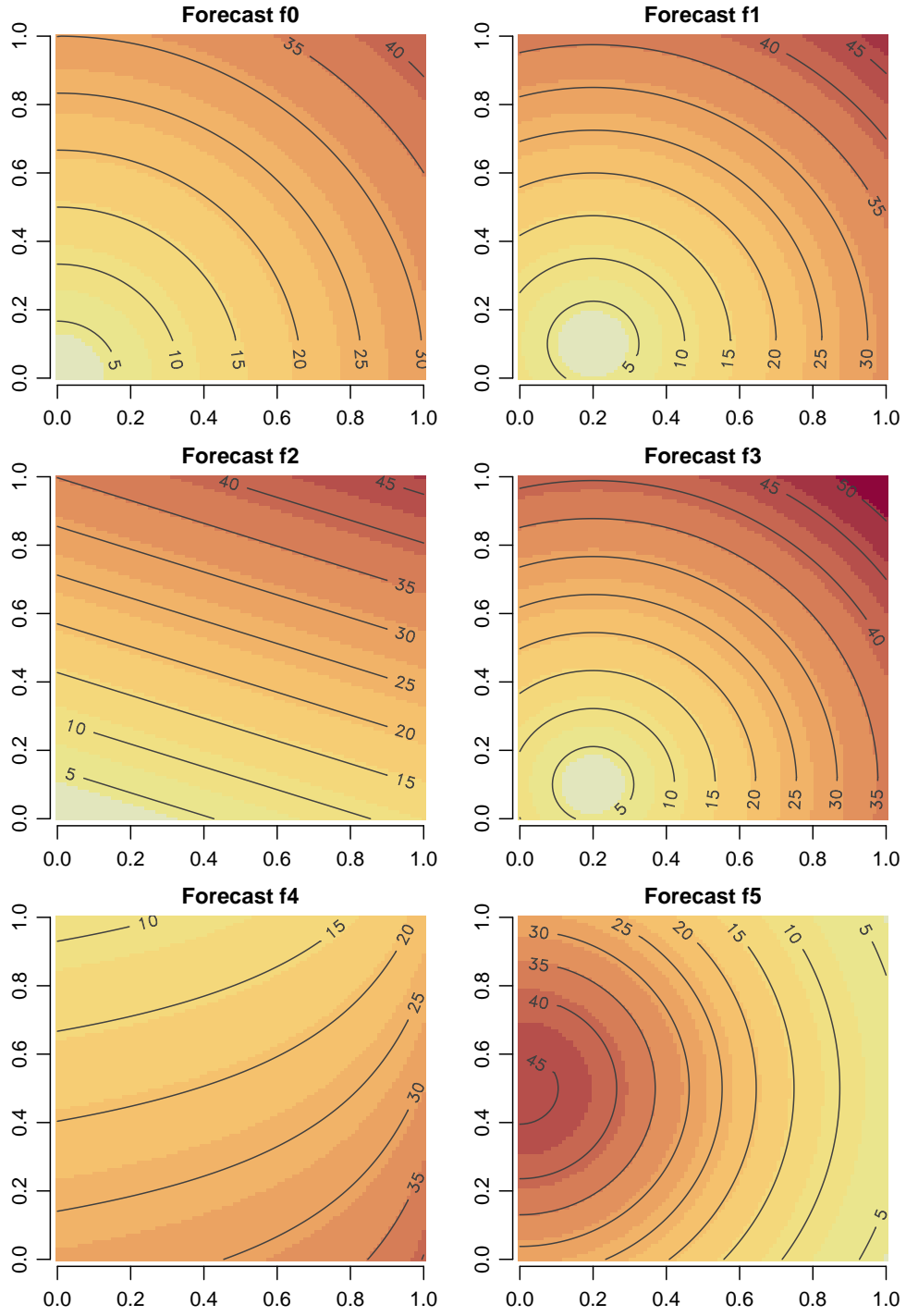


Figure 1: Heat maps of the intensity forecasts f_0, \dots, f_5 .

The motivation for this choice is as follows. Intensity f_1 is intuitively the best forecast since it has roughly the correct shape up to a small shift and f_3 is a version of f_1 with a too high scaling factor. Intensity f_2 is similar to f_0 but linear while f_4 and f_5 have completely different shape, see Figure 1 for an illustration. Except for f_3 , all intensities put roughly identical mass on $[0, 1]^2$. This allows for an assessment of how the scoring function reacts to misspecifications in scale instead of shape.

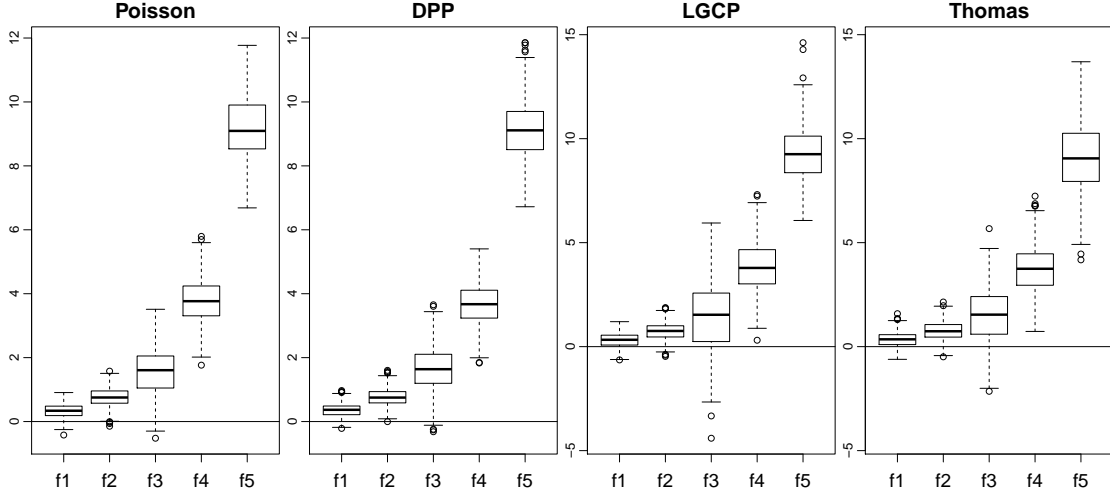


Figure 2: Boxplot of difference in average scores $\bar{s}_j - \bar{s}_0$ for $j = 1, \dots, 5$ and scoring function S_1 from Example 3.9. From left to right, Φ is a Poisson point process, a Gaussian determinantal point process, a log-Gaussian Cox process, or an inhomogeneous Thomas process.

Forecast comparison We begin with four simulation experiments based on the scoring function from Example 3.9, which we denote via S_1 in the following. The scaling factor $c > 0$ is chosen such that the logarithmic and squared terms are of the same order of magnitude in these simulations, giving $c = 0.1$. See Subsection 3.3 for a discussion of the choice of c .

In our first two experiments, Φ is a Poisson point process or a Gaussian determinantal point process, both having intensity λ . The latter is a determinantal point process (DPP) with Gaussian covariance, such that its points exhibit moderate inhibition. More details are given in Subsection 5.2 and Lavancier et al. (2015). The left part of Figure 2 shows the average score differences between the five different forecasts f_1, \dots, f_5 and the perfect forecast f_0 for both experiments. The plots show the same behaviour, namely f_1 is close to the optimal forecast, f_2 and f_3 are worse, and the average scores of the misspecified functions f_4 and f_5 are far from zero. Table 2 holds the results of DM tests (see Subsection 2.2) for both experiments. The rejection probabilities of f_0 against f_j , $j = 1, \dots, 5$ (first row) are overall in line with the average score differences in Figure 2. The only difference is that f_3 is less often deemed inferior to f_0 than f_2 , although it

Table 3: Fraction of times the ‘row forecast’ was preferred over the ‘column forecast’ by a standard DM test with level $\alpha = 0.05$, where Φ is a log-Gaussian Cox process (left) or an inhomogeneous Thomas process (right)

	f_0	f_1	f_2	f_3	f_4	f_5		f_0	f_1	f_2	f_3	f_4	f_5
f_0		0.30	0.62	0.28	0.98	1.00	f_0		0.25	0.49	0.36	0.95	1.00
f_1	0.00		0.33	0.26	0.82	1.00	f_1	0.01		0.24	0.34	0.79	1.00
f_2	0.00	0.01		0.17	0.72	1.00	f_2	0.00	0.00		0.20	0.68	1.00
f_3	0.00	0.00	0.01		0.19	0.95	f_3	0.01	0.01	0.02		0.26	0.95
f_4	0.00	0.00	0.00	0.01		0.99	f_4	0.00	0.00	0.00	0.01		0.97
f_5	0.00	0.00	0.00	0.00	0.00		f_5	0.00	0.00	0.00	0.00	0.00	

is clearly inferior to f_2 in terms of expected scores. A possible reason for this is the higher variance of the average score differences for f_3 compared to f_2 , as can be seen in Figure 2.

In the third and fourth simulation experiment Φ is a log-Gaussian Cox process (LGCP) or an inhomogeneous Thomas process, see e.g. Illian et al. (2008, Chapter 6). For the simulation of the LGCP, which has the intensity function

$$\lambda_{\text{LGCP}}(s) = \exp\left(\mu(s) + \frac{1}{2}C(s, s)\right) \quad (21)$$

for $s \in \mathbb{R}^2$, we chose the exponential covariance $C(s, t) = \frac{1}{4} \exp(-\|s - t\|^2)$ and μ such that $\lambda_{\text{LGCP}} = \lambda$ holds. The Thomas process is a cluster process which arises from an inhomogeneous Poisson process as parent and a random number of cluster points which are drawn from a normal distribution centered at its parent point. As intensity of the parent process we choose $\frac{\lambda}{2}$ and the number of points per cluster follow a Poisson distribution with parameter 2. The location of each cluster point is determined by a normal distribution which is centered at the parent point and where the components are uncorrelated and have standard deviation 0.05. As a result of the clustering, the intensity of the Thomas process is only approximately equal to λ .

The results of the third and fourth experiment are given in the right part of Figure 2. The overall behaviour of average score differences is the same as in the previous two experiments (same figure), but the variation increases, in particular for f_3 . As shown in Table 3, the results of DM tests are similar to the previous two experiments, as well, although the probabilities of preferring f_0 (first row) decrease substantially. An intuitive reason for this is that clustering, which is a feature of the LGCP and the Thomas process, complicates the distinction between different intensity forecasts. In contrast, the inhibition of the Gaussian DPP seems to facilitate the comparison, see Table 2. An increase in sample size from $N = 20$ to $N = 50$ can compensate for clustering and leads to more definitive preferring probabilities for the LGCP and Thomas process, as shown in Table 4.

Table 4: Fraction of times the ‘row forecast’ was preferred over the ‘column forecast’ by a standard DM test with level $\alpha = 0.05$, where Φ is a log-Gaussian Cox process (left) or an inhomogeneous Thomas process (right). In comparison to Table 3, the sample size was increased from $N = 20$ to $N = 50$

	f_0	f_1	f_2	f_3	f_4	f_5		f_0	f_1	f_2	f_3	f_4	f_5
f_0		0.49	0.91	0.50	1.00	1.00	f_0		0.43	0.80	0.56	1.00	1.00
f_1	0.00		0.60	0.46	0.99	1.00	f_1	0.00		0.41	0.57	0.99	1.00
f_2	0.00	0.00		0.25	0.99	1.00	f_2	0.00	0.00		0.28	0.94	1.00
f_3	0.00	0.00	0.01		0.32	1.00	f_3	0.00	0.00	0.00		0.48	1.00
f_4	0.00	0.00	0.00	0.00		1.00	f_4	0.00	0.00	0.00	0.00		1.00
f_5	0.00	0.00	0.00	0.00	0.00		f_5	0.00	0.00	0.00	0.00	0.00	

Relation to earthquake likelihood model testing We now investigate how the forecast comparison changes when using scoring functions motivated by earthquake likelihood model testing (Subsection 4.3) instead of S_1 from Example 3.9. We start with the scoring function (20), denote it via S_2 , and repeat the simulation experiments for the four different choices of Φ as above. Boxplots of average score differences are given in Figure 3 and they appear overall similar to the ones presented in Figure 2. A notable exception is the forecast f_3 , which attains much smaller score differences under S_2 compared to S_1 , and now seems preferable to f_2 . Inspecting the results of DM tests given in

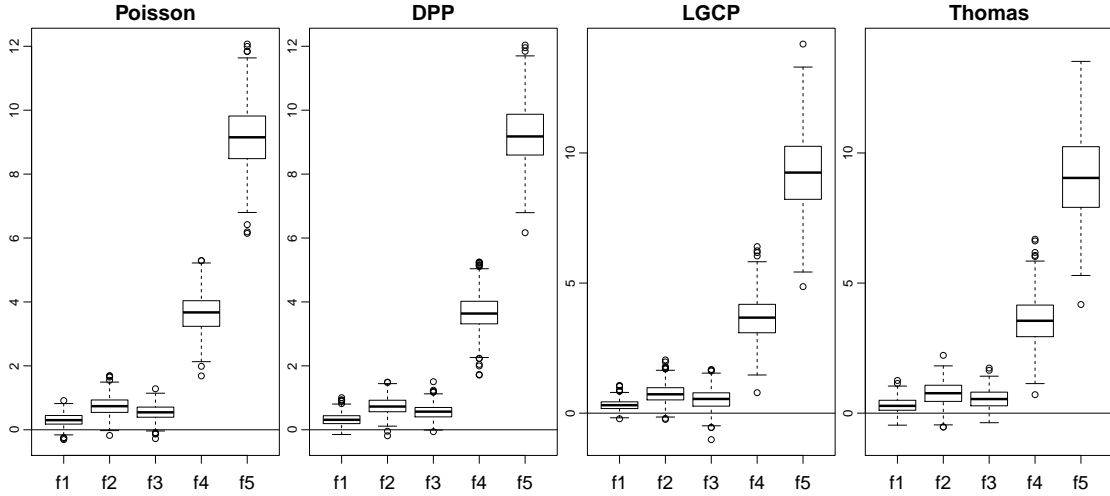


Figure 3: Boxplot of difference in average scores $\bar{s}_j - \bar{s}_0$ for $j = 1, \dots, 5$ and scoring function S_2 (see (20)). From left to right, Φ is a Poisson point process, a Gaussian determinantal point process, a log-Gaussian Cox process, or an inhomogeneous Thomas process.

Table 5 confirms this notion and reveals further noteworthy differences. If we compare the rows of f_0 and f_1 in Table 5 to the left-hand side of Table 2 and 3, we observe

Table 5: Fraction of times the ‘row forecast’ was preferred over the ‘column forecast’ by a standard DM test with level $\alpha = 0.05$ based on the scoring function S_2 (see (20)). Φ is a Poisson point process (left) or a log-Gaussian Cox process (right)

	f_0	f_1	f_2	f_3	f_4	f_5		f_0	f_1	f_2	f_3	f_4	f_5
f_0		0.50	0.83	0.75	1.00	1.00	f_0		0.44	0.70	0.47	1.00	1.00
f_1	0.00		0.42	0.61	0.99	1.00	f_1	0.00		0.38	0.26	0.98	1.00
f_2	0.00	0.00		0.01	0.96	1.00	f_2	0.00	0.00		0.04	0.91	1.00
f_3	0.00	0.00	0.12		0.99	1.00	f_3	0.00	0.01	0.12		0.89	1.00
f_4	0.00	0.00	0.00	0.00		1.00	f_4	0.00	0.00	0.00	0.00		1.00
f_5	0.00	0.00	0.00	0.00	0.00		f_5	0.00	0.00	0.00	0.00	0.00	

that the probabilities of preferring f_0 or f_1 are nearly everywhere higher for S_2 than for S_1 . This suggests that in our experiments S_2 is more suited than S_1 to distinguish the (nearly) optimal forecasts from the competitors. Moreover, if we compare the values corresponding to the pair f_2 and f_3 , we see that f_2 is more often preferred to f_3 under S_1 than vice versa. For S_2 the roles are switched and f_3 is now preferred to f_2 more often. Since f_3 is a wrongly scaled version of the ‘almost perfect’ forecast f_1 , a possible reason for this is that S_2 is less sensitive to scaling than S_1 . It puts more emphasis on the shape of the intensity at the cost of less sensitivity to the number of points. As in the previous experiments, the clustering of the LGCP leads to less conclusive decisions between the forecasts, see Table 5.

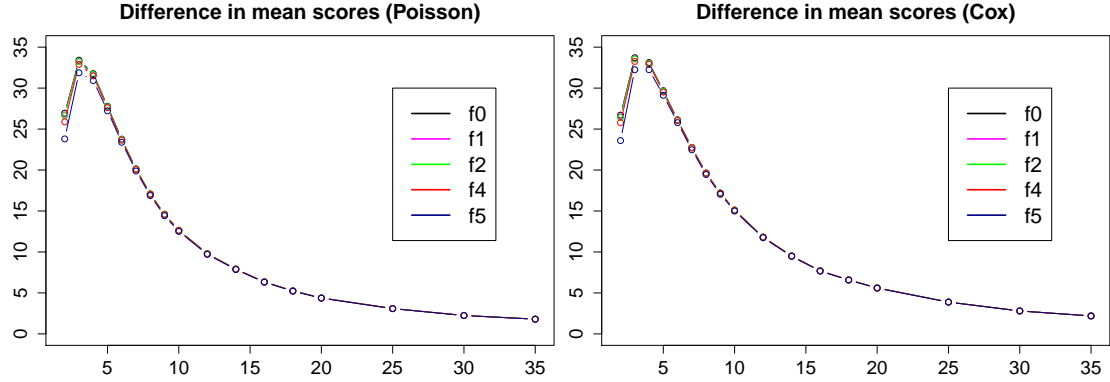


Figure 4: Average differences in realized scores $S_{\text{bin}}^{\mathcal{T}_n} - S_2 + C_n$ for different values of n , where C_n is a correction term as given in Proposition 4.4. The process Φ is a Poisson point process (left) or a log-Gaussian Cox process (right). Note that f_3 obtains the same values as f_1 since the difference $S_{\text{bin}}^{\mathcal{T}_n} - S_2$ is independent of the scaling of the reports.

A further sequence of experiments considers the speed of convergence in Proposition 4.4, i.e. how well the binned scoring function $S_{\text{bin}}^{\mathcal{T}_n}$ given in (18), together with a forecast-independent correction term, approximates S_2 . We select a dissecting system of partitions $(\mathcal{T}_n)_{n \in \mathbb{N}}$ of $[0, 1]^2$ which arises from partitioning both axes, i.e. each bin

$B_{ij}^{(n)} \in \mathcal{T}_n$ is given by $[(i-1)/n, i/n] \times [(j-1)/n, j/n]$ for $i, j \in \{1, \dots, n\}$. The number of bins is thus $k_n = n^2$ and we choose $n \in \{1, 2, \dots, 35\}$ for the simulations. As forecasts we rely on the functions f_0, \dots, f_5 introduced above which we transform into bin reports $f_{l,ij}^{(n)}$ by computing the integral of f_l over the bin $B_{ij}^{(n)}$ for all bins. These reports are then compared to the number of points per bin via $S_{\text{bin}}^{\mathcal{T}_n}$. Figure 4 illustrates convergence for growing n in the case where Φ is a Poisson process or a LGCP as specified above with $M = 200$ repetitions. It underlines that the speed of convergence depends on the reported intensity. The behaviour does not change significantly when using the Gaussian DPP or Thomas process, thus the corresponding plots are omitted.

An alternative way to study convergence consists of plotting the results of DM tests based on $S_{\text{bin}}^{\mathcal{T}_n}$ for increasing n . The corresponding fractions converge to the values in Table 5, as illustrated in Figure 5 for the comparisons of f_0 to f_1, \dots, f_4 . Note that f_5 is omitted in this figure, since f_0 was always preferred over f_5 for all values of n . These simulations suggest that starting from $n = 10$, i.e. for 100 bins, the DM results based on $S_{\text{bin}}^{\mathcal{T}_n}$ are overall in good agreement with the results based on S_2 .

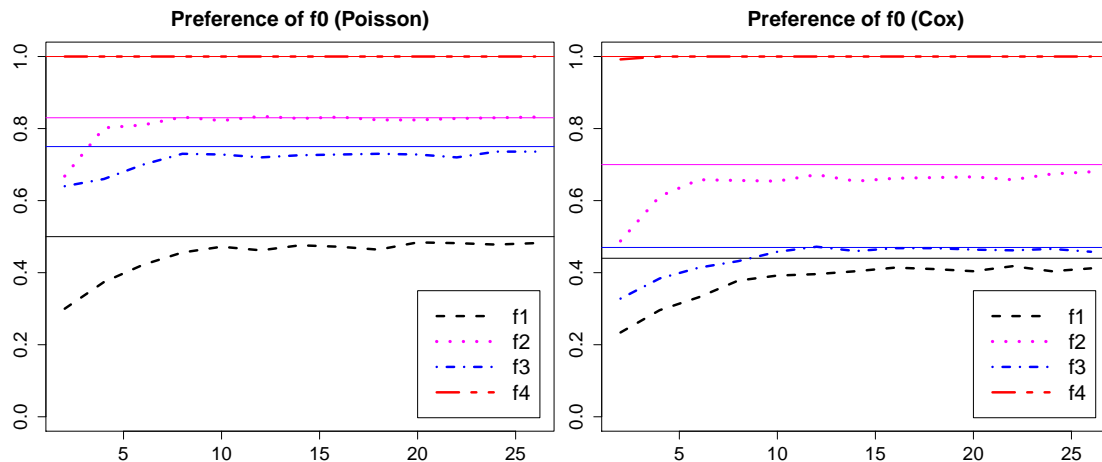


Figure 5: Fraction of times f_0 was preferred over f_1, \dots, f_4 by a standard DM test with level $\alpha = 0.05$ based on the scoring function $S_{\text{bin}}^{\mathcal{T}_n}$ and different n . The solid lines represent the fractions resulting from the use of S_2 (see (20)), as given in the first rows of Table 5. The process Φ is a Poisson point process (left) or a log-Gaussian Cox process (right).

5.2 Product density

In this subsection we focus on Scenario A again, however, we now consider second order properties and keep intensities fixed. We simulate a stationary and isotropic point processes Φ on the window $[0, 1]^2$ with three different second order structures corresponding to inhibition, clustering, and no interaction. We draw $N = 20$ i.i.d. samples φ_i from Φ and compare the average scores for different forecasts, in the same way as in the previous

subsection. The scoring function S is defined in Example 3.11 and the scaling factor $c > 0$ is chosen such that the log and squared terms are of the same order of magnitude, in this case $c = 10^{-5}$. We repeat the simulations $M = 500$ times to assess the variation in average scores.

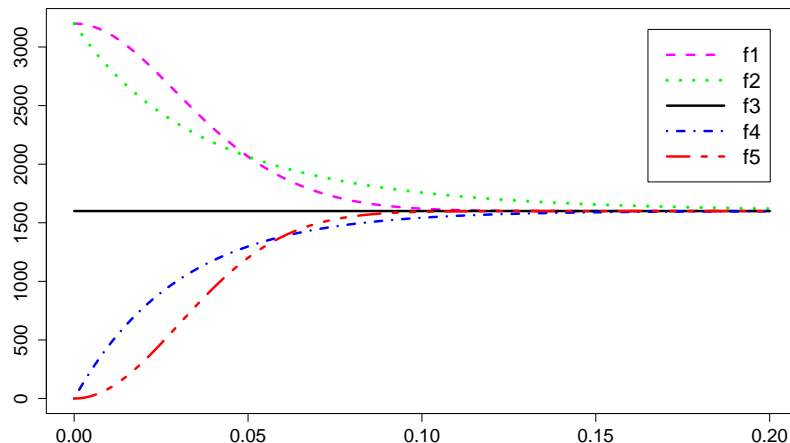


Figure 6: Plot of the five different product densities used as forecasts in Subsection 5.2.

Five different product density forecasts are compared below, given by

$$\begin{aligned} f_1(r) &= \exp \left(2\mu + \sigma^2 \left(1 + \exp(-400r^2) \right) \right) \\ f_2(r) &= \exp \left(2\mu + \sigma^2 \left(1 + \exp(-20r) \right) \right) \\ f_3(r) &= \lambda^2 \\ f_4(r) &= \lambda^2 \left(1 - \exp(-2r/\gamma) \right) \\ f_5(r) &= \lambda^2 \left(1 - \exp(-2(r/\gamma)^2) \right), \end{aligned}$$

where we choose $\mu = \log(\lambda) - \sigma^2/2$, $\sigma^2 = \log(2)$, $\gamma = 0.06$ and $\lambda = 40$. See Figure 6 for a graphical comparison of the different functions. The first two forecasts represent clustering, since they arise as product densities of log-Gaussian Cox processes (LGCPs). A stationary and isotropic LGCP is determined by a stationary and isotropic Gaussian process with mean μ and covariance function $C_0 : [0, \infty) \rightarrow \mathbb{R}$. Its second order product density $\varrho^{(2)}$ is of the form $\varrho^{(2)}(x_1, x_2) = \varrho_0^{(2)}(\|x_1 - x_2\|)$ with

$$\varrho_0^{(2)}(r) = \exp(2\mu + C_0(0) + C_0(r)),$$

see e.g. Illian et al. (2008). The forecasts f_1 and f_2 are the product densities of a LGCP with Gaussian and exponential covariance function, respectively. The variance and scale are chosen as $\sigma^2 = \log(2)$ and $s = 0.05$ in both cases.

The forecast f_3 corresponds to a homogeneous Poisson process. The remaining two forecasts arise as product densities of determinantal point processes (DPPs) and thus

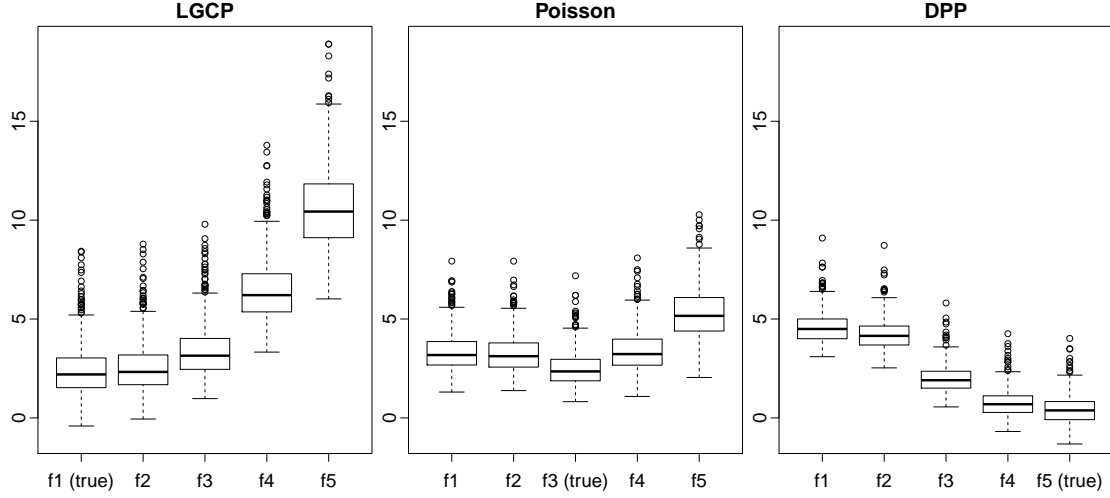


Figure 7: Boxplots of average scores \bar{s}_j for different product density forecasts, where Φ is a log-Gaussian Cox process (left), a homogeneous Poisson process (center), or a Gaussian determinantal point process (right).

represent inhibition. In general, a DPP is a locally finite point process with product densities given by

$$\rho^{(n)}(x_1, \dots, x_n) = \det(C(x_i, x_j))_{i,j=1, \dots, n} \quad (22)$$

for all $n \in \mathbb{N}$, where $C : \mathbb{R}^d \times \mathbb{R}^d \rightarrow \mathbb{R}$ is a covariance, see [Hough et al. \(2006\)](#) and [Lavancier et al. \(2015\)](#) for details. A DPP has intensity $x \mapsto C(x, x)$ and it is stationary and isotropic whenever its covariance is. In this case, we have $C(x, y) = C_0(\|x - y\|)$ for some $C_0 : [0, \infty) \rightarrow \mathbb{R}$ such that the second order product density is given by

$$\varrho_0^{(2)}(r) = C_0(0)^2 - C_0(r)^2.$$

The forecasts f_4 and f_5 are the product densities of a DPP with exponential and Gaussian covariance function, respectively. The variance and scale are chosen as $\lambda^2 = 40^2$ and $\gamma = 0.06$ in both cases. Our parameter choices ensure that the point process models corresponding to f_1, \dots, f_5 all have intensity equal to λ .

In the first experiment the true Φ is a LGCP with a Gaussian covariance function such that it has product density f_1 and intensity λ . In the second experiment Φ is a homogeneous Poisson process with intensity λ , such that f_3 becomes the perfect forecast in this situation. Lastly, we let Φ be a DPP with Gaussian covariance function and parameters such that f_5 is the optimal forecasts. We thus perform one experiment for each of the three phenomena clustering, no interaction, and inhibition.

The simulated average scores are displayed in Figure 7 for all three experiments. The optimal forecast consistently achieves the lowest average scores. In the case of clustering (left subfigure) the LGCP related forecasts f_1 and f_2 perform roughly similar, while the

Table 6: Fraction of times the ‘row forecast’ was preferred over the ‘column forecast’ by a standard DM test with level $\alpha = 0.05$. Φ is a log-Gaussian Cox process (left), a homogeneous Poisson process (center), or a Gaussian determinantal point process (right)

	f_1	f_2	f_3	f_4	f_5		f_1	f_2	f_3	f_4	f_5
f_1		0.23	0.73	1.00	1.00	f_1		0.00	0.00	0.00	0.00
f_2	0.01		0.64	1.00	1.00	f_2	0.97		0.00	0.00	0.00
f_3	0.00	0.00		1.00	1.00	f_3	1.00	1.00		0.00	0.00
f_4	0.00	0.00	0.00		1.00	f_4	1.00	1.00	1.00		0.00
f_5	0.00	0.00	0.00	0.00		f_5	1.00	1.00	1.00	0.70	

	f_1	f_2	f_3	f_4	f_5
f_1		0.01	0.00	0.05	0.66
f_2	0.21		0.00	0.06	0.73
f_3	0.91	0.85		0.85	1.00
f_4	0.07	0.05	0.00		1.00
f_5	0.00	0.00	0.00	0.00	

misspecified no interaction and inhibition forecasts f_3 , f_4 and f_5 lead to considerably higher average scores. A similar, but mirrored behavior is apparent in the inhibition experiment (right subfigure): The forecast f_4 , which gets the nature of point interactions right, attains low average scores, even though it is not optimal. The average scores of the Poisson forecast f_3 are always in between the ‘extremes’. The DM test probabilities of the three experiments are given in Table 6 and support these observations. Additionally, the DM results illustrate that the clustering forecasts f_1 and f_2 are preferred more often over the inhibition forecast f_5 in the case of Poisson data (center table).

5.3 Conditional intensity (temporal)

In this subsection we turn to Scenario B and simulate stationary Hawkes point processes (see Example 3.13) on an interval $[0, T]$ to compare forecasts of the conditional intensity. We compute realized scores with the scoring function S from Example 3.14 and divide them by the length of the interval T . Note that normalizing the score by the number of realized points is not feasible, as we want to retain (strict) consistency. We repeat the simulation $M = 500$ times to assess the variation in realized scores.

We compare five different conditional intensity reports of the form given in Example 3.13 and fix the background rate $\nu = 2$ such that the reports differ in the triggering functions only. We define five different triggering function forecasts given by

$$\begin{aligned}
 f_1(t) &= 2 \exp(-4t) \\
 f_2(t) &= 5/4 \exp(-2t) \\
 f_3(t) &= 2 \exp(-9/2t^2) \\
 f_4(t) &= 2 \max\{4 - 6t, 0\}
 \end{aligned}$$

$$f_5(t) = \mathbb{1}(t \in [0, 0.8])$$

We select f_1 and f_3 as candidates for the truth and let f_2, \dots, f_5 differ in shape. A graphical comparison of the functions is given in Figure 8.

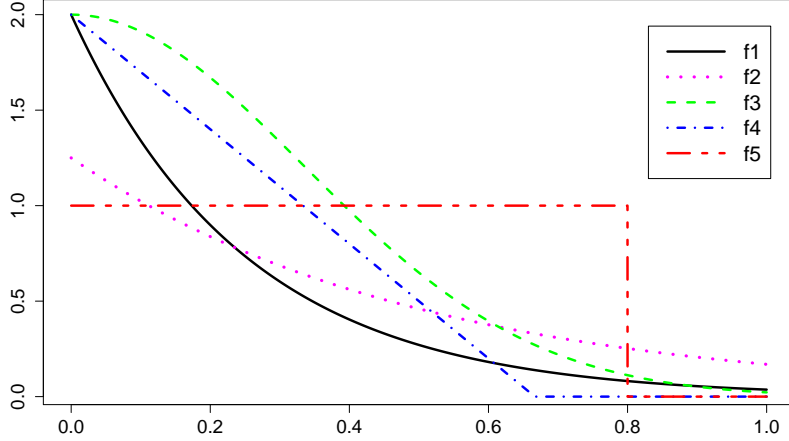


Figure 8: Plot of the five different triggering functions used as forecasts in Subsection 5.3.

Forecast comparison In our first two experiments, the true process Φ is a Hawkes process with triggering functions f_1 or f_3 . The left part of Figure 9 shows the corresponding boxplots for the score differences between the true forecast and the four competitors on the interval $[0, T]$. In both experiments the score differences are overall positive, such that the true forecast can be identified. Increasing the interval $[0, T]$ (not shown) does not change the overall appearance of the boxplots. However, the variance increases as we consider realized scores scaled by the interval length T instead of average scores.

Relation to information gain approach We now use the idea of information gains discussed in Subsection 4.1 as an alternative method to compare forecasts for the conditional intensity. To this end, we use the setting of Subsection 4.3 and let $(\mathcal{T}_n)_{n \in \mathbb{N}}$ be a family of partitions of $(0, T]$ which consist of intervals $(a_i^{(n)}, b_i^{(n)}] = ((i-1)T/n, iT/n]$ for $i = 1, \dots, n$. We again rely on the triggering functions f_1, \dots, f_5 introduced above and transform them into collections of conditional probabilities $p_{l,i}^{(n)}$ of points materializing in each interval via the formula in Proposition 4.1. These reports are then compared to the realized data via the scoring function $S_{\text{int}}^{\mathcal{T}_n}$ defined in (16). The right part of Figure 9 displays boxplots for $M = 500$ realized scores, where the interval $[0, 50]$ is partitioned into $n = 1000$ intervals. As in the first two experiments, f_1 and f_3 are the true triggering functions. The behavior of the realized scores closely resembles the left part of Figure 9, suggesting that for $n = 1000$ the forecast ranking based on $S_{\text{int}}^{\mathcal{T}_n}$ is a reasonable approximation to the one based on S .

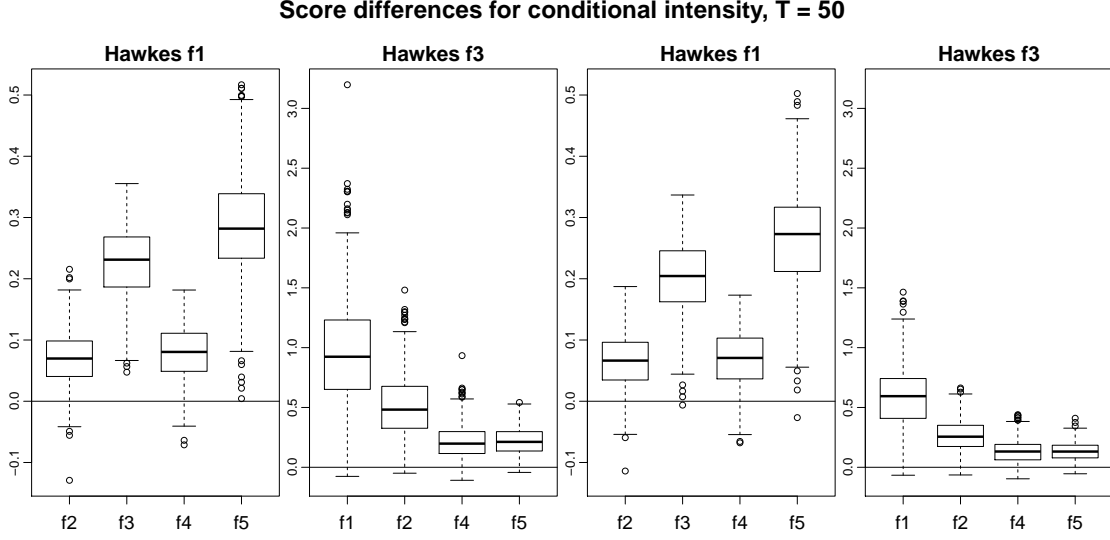


Figure 9: Boxplots of score differences between the true forecasts and the four remaining competitors, where Φ is a Hawkes process on the interval $[0, 50]$ with triggering function f_1 or f_3 . The two plots on the left show the scoring function S from Example 3.14 while the plots on the right show $S_{\text{int}}^{\mathcal{T}_n}$ (Equation (16)) with $n = 1000$.

Proposition 4.1 ensures that the scores computed from $S_{\text{int}}^{\mathcal{T}_n}$ converge to the realized scores under S if a suitable correction term is added. Figure 10 illustrates the speed of this convergence for different n based on the simulation of $M = 200$ samples and $T = 50$. It highlights that the speed of convergence depends on the underlying process. However, the absolute difference between $S_{\text{int}}^{\mathcal{T}_n}$ and S is less important than the overall forecast rankings of the scoring functions. As illustrated by Figure 9 these rankings are already in good agreement for $n = 1000$, i.e. an interval length of 0.05.

6 Discussion

Assessing forecast accuracy and comparing the performance of several competing forecasts is a non-trivial task that appears across multiple disciplines and sectors. When quantities of interest are real numbers, consistent scoring functions lie at the heart of theoretically underpinned techniques. In this article we show that consistent scoring functions transfer to the point process setting and are available for a variety of popular point process characteristics (Section 3). The corresponding model evaluation principles (Section 2) can improve forecast evaluation for point processes in a variety of applications and they naturally encompass several existing techniques for model comparison (Section 4). Simulation experiments illustrate that beyond their theoretical properties, consistent scoring functions are able to effectively compare forecasts based on finite sample sizes in some elementary settings (Section 5). We close with a discussion of how our setting relates to existing methods and a future outlook on possible refinements of

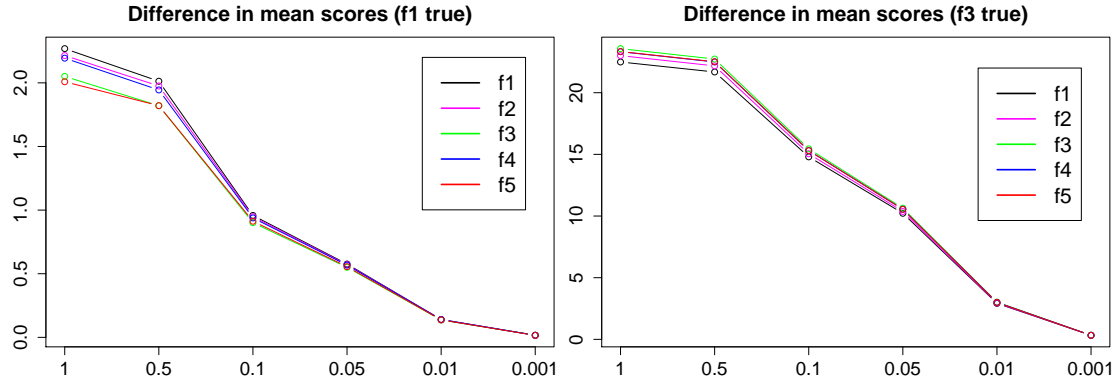


Figure 10: Average differences in realized scores $S_{\text{int}}^{\mathcal{T}_n} - S + C_n$ for different values of T/n , where C_n is a correction term as given in Proposition 4.1 and the scoring functions are defined in Equation (16) and Example 3.14, respectively. The process Φ is a Hawkes process with triggering function f_1 (left) or f_3 (right) on the interval $[0, 50]$.

scoring function-based forecast evaluation for point processes.

The report and comparison of point process characteristics, as emphasized in this manuscript, can be contrasted to the forecasting setting of Heinrich et al. (2019), who apply an estimator to each point pattern and then compare the resulting distributions in an ‘estimator space’ via consistent scoring functions for distributions. In practice such distributions will usually not be explicitly available and will only be accessible via simulations from the reported point process models. On the one hand, Heinrich et al. (2019) argue that their approach has better discrimination ability, as the whole point process distribution is taken into account. On the other hand, approximating the resulting scores via simulations leads to high computational costs, which might be prohibitive in routine evaluations. Moreover, when using characteristics such as the intensity, issuing a report is easier since the forecasters do not need to have a fully specified point process model in mind. Overall, we think that the scoring functions proposed in this manuscript provide a crucial complement to Heinrich et al. (2019) and whichever approach is more suitable will likely depend on the problem at hand.

The central use of scoring functions, as discussed in Section 2, is the comparison of (at least) two competing models or forecasts. It thus contrasts with many existing point process model evaluation tools, which focus on absolute performance and goodness-of-fit. Prominent examples are point process residuals, which form an empirical process arising from fitting a conditional intensity to data (Schoenberg, 2003; Baddeley et al., 2005; Bray et al., 2014) and evaluation methods based on summary statistics, see e.g. Bray and Schoenberg (2013). Moreover, Thorarinsdottir (2013) transfers the probability integral transform (PIT) to the point process setting in order to measure forecast calibration (Dawid, 1984). Although both, absolute and relative performance evaluation, are important in choosing suitable models, a selection among the available competitors has to be done eventually, and measures of absolute performance are not designed, and hence

often badly positioned, for such a choice. Moreover, as pointed out by [Nolde and Ziegel \(2017\)](#), focusing on absolute performance measures may lead to wrong incentives in designing candidate models. Hence, consistent scoring functions for point processes are not competing with existing absolute performance measures, but are a useful additional tool.

Several results are available to tailor scoring functions to certain practical applications or address further issues in comparing forecast performance. Firstly, *weighted scoring functions* provide a way to emphasize forecast performance on regions of interest and ignore it on others. [Lerch et al. \(2017\)](#) illustrate that a simple weighing of the realized scores can be misleading and [Holzmann and Klar \(2017\)](#) provide a general construction principle which ensures consistency. While previous work focuses mainly on the tails of the distribution, weighted scoring functions for point processes might focus on some spatial area or on the distribution of certain marks. Secondly, there are situations where the statistical property of interest cannot be computed explicitly from a model and is only accessible via simulations. In this case it is intuitive to use simulated realizations in order to approximate the realized score of the forecasts. This idea is a central element of the model comparison approach of [Heinrich et al. \(2019\)](#). *Fair versions* of consistent scoring functions aim to reduce a possible bias which might occur in such approximations, see e.g. [Ferro \(2014\)](#) for an overview. [Krüger et al. \(2021\)](#) address this issue when the model simulation is done via Markov chain Monte Carlo. Adapting these methods for point processes will enhance the usefulness of scoring functions for many applications.

Based on the results of this manuscript, consistent scoring functions for point processes and the methods relying on them present themselves as valuable tools in evaluating point process forecasts and choosing suitable models. Since we focus on working out the theoretical foundation, there are several avenues for future work. A first important task are investigations concerning the choice of scoring functions, including, but not limited to, simulation studies as in Section 5 to improve the understanding of finite sample behavior. Moreover, implementing the here proposed methods for specific applications poses highly relevant further problems, in particular if refinements such as suitable weighting or approximations are necessary. We thus anticipate model and forecast evaluation for point processes to remain an area of active research.

Acknowledgments

Jonas Brehmer and Tilmann Gneiting are grateful for support by the Klaus Tschira Foundation. Jonas Brehmer gratefully acknowledges support by the German Research Foundation (DFG) through Research Training Group RTG 1953. We thank Claudio Heinrich and Christopher Dörr for helpful discussions and remarks.

References

Anscombe, F. J. (1952). Large-sample theory of sequential estimation. *Proc. Cambridge*

- Philos. Soc.*, 48, 600–607. URL <https://doi.org/10.1017/s0305004100076386>.
- Baddeley, A., Rubak, E. and Turner, R. (2015). *Spatial Point Patterns: Methodology and Applications with R*. Chapman and Hall/CRC Press, London.
- Baddeley, A. and Turner, R. (2005). spatstat: An R package for analyzing spatial point patterns. *J. Stat. Softw.*, 12, 1–42. URL <https://www.jstatsoft.org/v012/i06>.
- Baddeley, A., Turner, R., Møller, J. and Hazelton, M. (2005). Residual analysis for spatial point processes. *J. R. Stat. Soc. Ser. B Stat. Methodol.*, 67, 617–666. With discussion and a reply by the authors, URL <https://doi.org/10.1111/j.1467-9868.2005.00519.x>.
- Barthelmé, S., Trukenbrod, H., Engbert, R. and Wichmann, F. (2013). Modeling fixation locations using spatial point processes. *J. Vis.*, 13, 1–34. URL <https://doi.org/10.1167/13.12.1>.
- Bray, A. and Schoenberg, F. P. (2013). Assessment of point process models for earthquake forecasting. *Statist. Sci.*, 28, 510–520. URL <https://doi.org/10.1214/13-STS440>.
- Bray, A., Wong, K., Barr, C. D. and Schoenberg, F. P. (2014). Voronoi residual analysis of spatial point process models with applications to California earthquake forecasts. *Ann. Appl. Stat.*, 8, 2247–2267. URL <https://doi.org/10.1214/14-AOAS767>.
- Chen, J., Hawkes, A. G., Scalas, E. and Trinh, M. (2018). Performance of information criteria for selection of Hawkes process models of financial data. *Quant. Finance*, 18, 225–235. URL <https://doi.org/10.1080/14697688.2017.1403140>.
- Chiu, S. N., Stoyan, D., Kendall, W. S. and Mecke, J. (2013). *Stochastic geometry and its applications*. 3rd ed. Wiley Series in Probability and Statistics, John Wiley & Sons, Ltd., Chichester. URL <https://doi.org/10.1002/9781118658222>.
- Clements, R. A., Schoenberg, F. P. and Schorlemmer, D. (2011). Residual analysis methods for space-time point processes with applications to earthquake forecast models in California. *Ann. Appl. Stat.*, 5, 2549–2571. URL <https://doi.org/10.1214/11-AOAS487>.
- Daley, D. J. and Vere-Jones, D. (2003). *An introduction to the theory of point processes. Vol. I*. 2nd ed. Probability and its Applications (New York), Springer-Verlag, New York. Elementary theory and methods.
- Daley, D. J. and Vere-Jones, D. (2004). Scoring probability forecasts for point processes: the entropy score and information gain. *J. Appl. Probab.*, 41A, 297–312. Stochastic methods and their applications, URL <https://doi.org/10.1239/jap/1082552206>.
- Dawid, A. P. (1984). Statistical theory. The prequential approach. *J. Roy. Statist. Soc. Ser. A*, 147, 278–292. URL <https://doi.org/10.2307/2981683>.

- Dawid, A. P., Lauritzen, S. and Parry, M. (2012). Proper local scoring rules on discrete sample spaces. *Ann. Statist.*, 40, 593–608. URL <https://doi.org/10.1214/12-AOS972>.
- Dawid, A. P. and Musio, M. (2014). Theory and applications of proper scoring rules. *Metron*, 72, 169–183. URL <https://doi.org/10.1007/s40300-014-0039-y>.
- Dawid, A. P. and Sebastiani, P. (1999). Coherent dispersion criteria for optimal experimental design. *Ann. Statist.*, 27, 65–81. URL <https://doi.org/10.1214/aos/1018031101>.
- Diebold, F. X. and Mariano, R. S. (1995). Comparing predictive accuracy. *J. Bus. Econom. Statist.*, 13, 253–263. URL <https://doi.org/10.1198/073500102753410444>.
- Ehm, W. and Gneiting, T. (2012). Local proper scoring rules of order two. *Ann. Statist.*, 40, 609–637. URL <https://doi.org/10.1214/12-AOS973>.
- Embrechts, P., Klüppelberg, C. and Mikosch, T. (1997). *Modelling extremal events*, vol. 33 of *Applications of Mathematics (New York)*. Springer-Verlag, Berlin. For insurance and finance, URL <https://doi.org/10.1007/978-3-642-33483-2>.
- Ferro, C. A. T. (2014). Fair scores for ensemble forecasts. *Q.J.R. Meteorol. Soc.*, 140, 1917–1923. URL <https://doi.org/10.1002/qj.2270>.
- Field, E. H. (2007). Overview of the working group for the development of regional earthquake likelihood models (RELM). *Seismol. Res. Lett.*, 78, 7–16. URL <https://doi.org/10.1785/gssrl.78.1.7>.
- Fissler, T. and Ziegel, J. F. (2016). Higher order elicibility and Osband’s principle. *Ann. Statist.*, 44, 1680–1707. URL <https://doi.org/10.1214/16-AOS1439>.
- Flaxman, S., Chirico, M., Pereira, P. and Loeffler, C. (2019). Scalable high-resolution forecasting of sparse spatiotemporal events with kernel methods: A winning solution to the NIJ “Real-Time Crime Forecasting Challenge”. *Ann. Appl. Stat.*, 13, 2564–2585. URL <https://doi.org/10.1214/19-aos1284>.
- Fox, E. W., Short, M. B., Schoenberg, F. P., Coronges, K. D. and Bertozzi, A. L. (2016). Modeling e-mail networks and inferring leadership using self-exciting point processes. *J. Amer. Statist. Assoc.*, 111, 564–584. URL <https://doi.org/10.1080/01621459.2015.1135802>.
- Frongillo, R. and Kash, I. A. (2015). Vector-valued property elicitation. *J. Mach. Learn. Res. Workshop Conf. Proc.*, 40, 1–18. URL <https://www.cs.colorado.edu/~raf/media/papers/vec-props.pdf>.
- Frongillo, R. and Kash, I. A. (2021). Elicitation complexity of statistical properties. *Biometrika*. In press, URL <https://doi.org/10.1093/biomet/asaa093>.

- Giacomini, R. and White, H. (2006). Tests of conditional predictive ability. *Econometrica*, 74, 1545–1578. URL <http://dx.doi.org/10.1111/j.1468-0262.2006.00718.x>.
- Gneiting, T. (2011). Making and evaluating point forecasts. *J. Amer. Statist. Assoc.*, 106, 746–762. URL <https://doi.org/10.1198/jasa.2011.r10138>.
- Gneiting, T. and Raftery, A. E. (2007). Strictly proper scoring rules, prediction, and estimation. *J. Amer. Statist. Assoc.*, 102, 359–378. URL <https://doi.org/10.1198/016214506000001437>.
- Gneiting, T. and Ranjan, R. (2011). Comparing density forecasts using threshold- and quantile-weighted scoring rules. *J. Bus. Econom. Statist.*, 29, 411–422. URL <https://doi.org/10.1198/jbes.2010.08110>.
- Harte, D. (2015). Log-likelihood of earthquake models: evaluation of models and forecasts. *Geophys. J. Int.*, 201, 711–723. URL <https://doi.org/10.1093/gji/ggu442>.
- Harte, D. and Vere-Jones, D. (2005). The entropy score and its uses in earthquake forecasting. *Pure Appl. Geophys.*, 162, 1229–1253. URL <https://doi.org/10.1007/s00024-004-2667-2>.
- Hawkes, A. G. (1971). Spectra of some self-exciting and mutually exciting point processes. *Biometrika*, 58, 83–90. URL <https://doi.org/10.1093/biomet/58.1.83>.
- Heinrich, C., Schneider, M., Guttorp, P. and Thorarinsdottir, T. (2019). Validation of point process forecasts. Preprint, URL <https://www.nr.no/en/nrpublication?query=/file/1564572954/PointProcessValidation-Heinrich.pdf>.
- Hendrickson, A. D. and Buehler, R. J. (1971). Proper scores for probability forecasters. *Ann. Math. Statist.*, 42, 1916–1921. URL <https://doi.org/10.1214/aoms/1177693057>.
- Holzmann, H. and Klar, B. (2017). Focusing on regions of interest in forecast evaluation. *Ann. Appl. Stat.*, 11, 2404–2431. URL <https://doi.org/10.1214/17-A0AS1088>.
- Hough, J. B., Krishnapur, M., Peres, Y. and Virág, B. (2006). Determinantal processes and independence. *Probab. Surv.*, 3, 206–229. URL <https://doi.org/10.1214/154957806000000078>.
- Hwang, E. and Shin, D. W. (2012). Random central limit theorems for linear processes with weakly dependent innovations. *J. Korean Statist. Soc.*, 41, 313–322. URL <https://doi.org/10.1016/j.jkss.2011.10.004>.
- Hyvärinen, A. (2005). Estimation of non-normalized statistical models by score matching. *J. Mach. Learn. Res.*, 6, 695–709. URL <https://jmlr.org/papers/v6/hyvarinen05a.html>.

- Illian, J., Penttinen, A., Stoyan, H. and Stoyan, D. (2008). *Statistical analysis and modelling of spatial point patterns*. Statistics in Practice, John Wiley & Sons, Ltd., Chichester.
- Kagan, Y. Y. and Jackson, D. D. (1995). New seismic gap hypothesis: Five years after. *J. Geophys. Res. Solid Earth*, 100, 3943–3959. URL <https://agupubs.onlinelibrary.wiley.com/doi/abs/10.1029/94JB03014>.
- Krüger, F., Lerch, S., Thorarinsdottir, T. L. and Gneiting, T. (2021). Predictive inference based on Markov chain Monte Carlo output. *Int. Stat. Rev.* In press, URL <https://doi.org/10.1111/insr.12405>.
- Lavancier, F., Møller, J. and Rubak, E. (2015). Determinantal point process models and statistical inference. *J. R. Stat. Soc. Ser. B. Stat. Methodol.*, 77, 853–877. URL <https://doi.org/10.1111/rssb.12096>.
- Lee, S. (1997). Random central limit theorem for the linear process generated by a strong mixing process. *Statist. Probab. Lett.*, 35, 189–196. URL [https://doi.org/10.1016/S0167-7152\(97\)00013-8](https://doi.org/10.1016/S0167-7152(97)00013-8).
- Lerch, S., Thorarinsdottir, T. L., Ravazzolo, F. and Gneiting, T. (2017). Forecaster’s dilemma: extreme events and forecast evaluation. *Statist. Sci.*, 32, 106–127. URL <https://doi.org/10.1214/16-STS588>.
- Marzocchi, W., Zechar, J. D. and Jordan, T. H. (2012). Bayesian forecast evaluation and ensemble earthquake forecasting. *Bull. Seismol. Soc. Amer.*, 102, 2574–2584. URL <https://doi.org/10.1785/0120110327>.
- Meyer, S. and Held, L. (2014). Power-law models for infectious disease spread. *Ann. Appl. Stat.*, 8, 1612–1639. URL <https://doi.org/10.1214/14-AOAS743>.
- Mikosch, T. (2009). *Non-life insurance mathematics*. 2nd ed. Universitext, Springer-Verlag, Berlin. An introduction with the Poisson process, URL <https://doi.org/10.1007/978-3-540-88233-6>.
- Mohler, G. O., Short, M. B., Brantingham, P. J., Schoenberg, F. P. and Tita, G. E. (2011). Self-exciting point process modeling of crime. *J. Amer. Statist. Assoc.*, 106, 100–108. URL <https://doi.org/10.1198/jasa.2011.ap09546>.
- Nolde, N. and Ziegel, J. F. (2017). Elicitability and backtesting: perspectives for banking regulation. *Ann. Appl. Stat.*, 11, 1833–1874. URL <https://doi.org/10.1214/17-AOAS1041>.
- Ogata, Y. (1981). On Lewis’ simulation method for point processes. *IEEE Trans. Inf. Theor.*, 27, 23–31. URL <https://doi.org/10.1109/TIT.1981.1056305>.
- Ogata, Y. (1998). Space-time point-process models for earthquake occurrences. *Ann. Inst. Statist. Math.*, 50, 379–402. URL <https://doi.org/10.1023/A:1003403601725>.

- Ogata, Y. and Tanemura, M. (1984). Likelihood analysis of spatial point patterns. *J. Roy. Statist. Soc. Ser. B*, 46, 496–518. URL www.jstor.org/stable/2345690.
- Peng, R. D., Schoenberg, F. P. and Woods, J. A. (2005). A space-time conditional intensity model for evaluating a wildfire hazard index. *J. Amer. Statist. Assoc.*, 100, 26–35. URL <https://doi.org/10.1198/016214504000001763>.
- R Core Team (2020). *R: A Language and Environment for Statistical Computing*. R Foundation for Statistical Computing, Vienna, Austria. URL <https://www.R-project.org/>.
- Reinhart, A. (2018). A review of self-exciting spatio-temporal point processes and their applications. *Statist. Sci.*, 33, 299–318. URL <https://doi.org/10.1214/17-STS629>.
- Rhoades, D., Schorlemmer, D., Gerstenberger, M., Christophersen, A., Zechar, J. D. and Imoto, M. (2011). Efficient testing of earthquake forecasting models. *Acta Geophys.*, 59, 728–747. URL <https://doi.org/10.2478/s11600-011-0013-5>.
- Savage, L. J. (1971). Elicitation of personal probabilities and expectations. *J. Amer. Statist. Assoc.*, 66, 783–801. URL <https://doi.org/10.2307/2284229>.
- Schoenberg, F. P. (2003). Multidimensional residual analysis of point process models for earthquake occurrences. *J. Amer. Statist. Assoc.*, 98, 789–795. URL <https://doi.org/10.1198/016214503000000710>.
- Schoenberg, F. P., Hoffmann, M. and Harrigan, R. J. (2019). A recursive point process model for infectious diseases. *Ann. Inst. Statist. Math.*, 71, 1271–1287. URL <https://doi.org/10.1007/s10463-018-0690-9>.
- Schorlemmer, D., Gerstenberger, M., Wiemer, S. and Jackson, D. (2007). Earthquake likelihood model testing. *Seismol. Res. Lett.*, 78, 17–29. URL <https://doi.org/10.1785/gssrl.78.1.17>.
- Schorlemmer, D. and Gerstenberger, M. C. (2007). RELM testing center. *Seismol. Res. Lett.*, 78, 30–36. URL <https://doi.org/10.1785/gssrl.78.1.30>.
- Schorlemmer, D., Werner, M. J., Marzocchi, W., Jordan, T. H., Ogata, Y., Jackson, D. D., Mak, S., Rhoades, D. A., Gerstenberger, M. C., Hirata, N., Liukis, M., Maechling, P. J., Strader, A., Taroni, M., Wiemer, S., Zechar, J. D. and Zhuang, J. (2018). The collaboratory for the study of earthquake predictability: Achievements and priorities. *Seismol. Res. Lett.*, 89, 1305–1313. URL <https://doi.org/10.1785/0220180053>.
- Shang, Y. (2012). A central limit theorem for randomly indexed m -dependent random variables. *Filomat*, 26, 713–717. URL <https://doi.org/10.2298/FIL1204713S>.
- Steinwart, I., Pasin, C., Williamson, R. and Zhang, S. (2014). Elicitation and identification of properties. *J. Mach. Learn. Res. Workshop Conf. Proc.*, 35, 1–45. URL <http://proceedings.mlr.press/v35/steinwart14.html>.

- Stoyan, D. and Penttinen, A. (2000). Recent applications of point process methods in forestry statistics. *Statist. Sci.*, 15, 61–78. URL <https://doi.org/10.1214/ss/1009212674>.
- Strader, A., Schneider, M. and Schorlemmer, D. (2017). Prospective and retrospective evaluation of five-year earthquake forecast models for California. *Geophys. J. Int.*, 211, 239–251. URL <https://doi.org/10.1093/gji/ggx268>.
- Taylor, S. W., Woolford, D. G., Dean, C. B. and Martell, D. L. (2013). Wildfire prediction to inform fire management: statistical science challenges. *Statist. Sci.*, 28, 586–615. URL <https://doi.org/10.1214/13-STS451>.
- Thorarinsdottir, T. L. (2013). Calibration diagnostic for point process models via the probability integral transform. *Stat*, 2, 150–158. URL <https://doi.org/10.1002/sta4.25>.
- Vere-Jones, D. (1998). Probability and information gain for earthquake forecasting. *Comput. Seismol.*, 30, 248–263. URL <https://doi.org/10.1029/CS005p0104>.
- Xu, H. and Schoenberg, F. P. (2011). Point process modeling of wildfire hazard in Los Angeles County, California. *Ann. Appl. Stat.*, 5, 684–704. URL <https://doi.org/10.1214/10-A0AS401>.
- Zechar, J. D., Gerstenberger, M. C. and Rhoades, D. A. (2010). Likelihood-based tests for evaluating space–rate–magnitude earthquake forecasts. *Bull. Seismol. Soc. Amer.*, 100, 1184–1195. URL <https://doi.org/10.1785/0120090192>.
- Zhuang, J., Ogata, Y. and Vere-Jones, D. (2002). Stochastic declustering of space-time earthquake occurrences. *J. Amer. Statist. Assoc.*, 97, 369–380. URL <https://doi.org/10.1198/016214502760046925>.